CONTROLLED SOURCE METHODS

CONTROLLED SOURCE ELECTRICAL METHODS (CSEM)

by

Stanley H. Ward

Earth Science Laboratory Division
University of Utah Research Institute
and
Department of Geology and Geophysics
University of Utah

TABLE OF CONTENTS

ABSTRACT

The objective of this manuscript is to sketch the problems inherent in application of controlled source electrical methods (CSEM) to crustal studies including mining, geothermal, sedimentary basin, and deep crustal/upper mantle exploration with focus on the latter. Measurements have been made in both the time and frequency domains with time domain measurements currently enjoying an advantage over frequency domain measurements for shallow applications.

Application of CSEM methods is impeded by natural field, electrification, geological, cultural, and topographic noise. Lateral resolution of parameters of adjacent steeply dipping bodies and vertical resolution of parameters of adjacent beds in a flatly dipping sequence are concerns with any CSEM method. Current channeling into a localized good conductor from a surrounding, overlying, or underlying conductor poses problems for the interpreter. Electromagnetic coupling is a problem specific to the resistivity and induced polarization methods.

In selecting a transmitter-receiver configuration for CSEM in a particular application, a compromise is usually achieved between such factors as domain of data acquisition, rejection of noise, resolution, current channeling, and depth of exploration. Not surprisingly there is only marginal agreement on the optimum selection of each of these variables for any given application. However, one of the more promising techniques for broad application in mining, geothermal, and sedimentary basin exploration is the controlled source audiomagnetotelluric method (CSAMT).

CSAMT is directly related to the grounded bipole method commonly used in deep crustal exploration. A summary of the results of several recent experiments with CSEM techniques illustrates that with care and difficulty they can be used to depths on the order of 20 km. An inductive loop source would seem to be preferred to a grounded bipole for this purpose if screening by a thick uniform conductive overburden is a problem. On the other hand, if measurements are made on a relatively uniform resistive surface, as can be found in glaciated Precambrian terranes, then either a grounded bipole or a loop source is acceptable. Most of the recent CSEM experiments were made over resistive Precambrian rocks and all were directed toward detecting a conductive layer at about 20 km depth. However, for exploration beyond this depth, the MT/AMT method would seem to be preferred. The rationale behind this conclusion is largely contained in consideration of the ratio of signal to noise. Where thick irregular surficial overburden of low resistivity occurs, two- and three-dimensional modeling is necessary to strip off the effects of the shallow layers. This may not be possible for CSEM and then MT/AMT becomes the only alternative.

INTRODUCTION

Controlled source electrical methods (CSEM) are applied in mining, geothermal, sedimentary basin, and deep crustal/upper mantle exploration. In this manuscript the problems inherent in controlled source electromagnetic, resistivity, and induced polarization methods are described with particular reference to mining exploration, the field in which electrical methods have been most refined. The problems include lateral and vertical resolution, current channeling, and natural field, electrification, geological, cultural, and topographic noise for all CSEM techniques. Electromagnetic coupling is an additional problem in resistivity and induced polarization surveys. Where pertinent, the implication of each of these problems is extended to deep crustal/upper mantle exploration with CSEM.

Whenever CSEM are to be used, whatever the scale of the problem, care must be exercised in selecting the optimum transmitter-receiver configuration. Factors to be considered include domain of data acquisition, rejection of noise, resolution, current channeling, and depth of exploration. Means for evaluating all of these factors objectively is not always at our disposal and hence, not surprisingly, there is only marginal agreement on the optimum system for any given application. One of the relatively new techniques for broad application in mining, geothermal, and sedimentary basins is the controlled source audiomagnetotelluric method (CSAMT). It is related to the grounded bipole method commonly used in deep crustal exploration.

After treating the problems of CSEM, and discussing the basis for selecting an optimum system for a given application, recent results using CSEM in deep crustal/upper mantle studies are summarized. A conductive horizon at

a depth of about 20 km is commonplace in these studies, yet it is difficult to be certain of its geological meaning. Most of these studies have been conducted over resistive Precambrian terranes. When one attempts to apply CSEM to unravel geological problems in terranes where heterogeneous conductive geological materials exist near surface, deep crustal and upper mantle exploration by CSEM becomes problematical unless one fortuitously acquires the use of a transmission line hundreds of kilometers in length. Even then, two- and three-dimensional earths must be used in interpretation. We conclude by demonstrating, via some simple models, the pitfalls of this approach.

PROBLEMS WITH INDUCTIVE CSEM SYSTEM

Overview

Figure 1 illustrates a typical geoelectric section to explore for economic mineral deposits via use of an inductive electromagnetic method. As depicted, a primary voltage (E) at the receiver is due solely to direct induction of the primary or transmitted alternating magnetic field. Superimposed on this primary voltage is a secondary voltage (ΔE) due to alternating magnetic fields arising in induced currents flowing in the assemblage of conductive media in the subsurface geoelectric section. From ΔE, or from $\frac{\Delta E}{E}$, the intention is to extract information about the massive sulfide body, i.e., its depth, depth extent, dip, strike, strike length, and its conductivity-thickness product. Most times this intent is satisfied, but in some instances it cannot be because the induction numbers θ_i for each member of the geoelectric section are too similar. As an illustration, one would hope that the following inequality holds:

$$\theta_1 = \sigma_1 \mu_1 \omega t_1 L \ll \theta_2 = \sigma_2 \mu_2 \omega t_2 L \quad . \qquad (1)$$

In equation (1) σ, μ, ω, and t are the conductivity, magnetic permeability, angular frequency, and thickness for the overburden (subscript 1) and the orebody (subscript 2). The parameter L is the separation between transmitting and receiving coils. If this inequality holds, then the contribution of the orebody can be clearly distinguished from the contribution of the overburden, in ΔE, provided all other induction numbers are much less than θ_1. As might be expected, the various θ_i are not always far apart with the result that separation of the contributions of the various elements of the geoelectric section to ΔE is not clear-cut. In addition, interactions between the elements of the geoelectric section can and do take place, e.g., current

channeling into a highly conductive medium from a less conductive medium. Nevertheless, the ultimate objective posed for any purely inductive electromagnetic method is to diagnose the parameters of each member of the geoelectric section from ΔE observed at surface. For grounded electromagnetic, resistivity, and induced polarization techniques, the ultimate objective is the same.

Unfortunately, a number of problems with all CSEM methods hinders the realization of the ultimate objective. Referring again to the inductive electromagnetic search problem of Figure 1, we can list the major problems rather readily as we have done in Table 1. In the ensuing, we shall address each of these problems in turn and make our suggestions for their minimization.

Natural field noise

Figure 2 illustrates a typical natural magnetic field spectrum. It exhibits field strength characteristics as follows: a low near 3 Hz, a rapid increase with decrease in frequency below 3 Hz, an interim peak near 100 Hz, and a trough near 1000 Hz followed by a rise at higher frequencies. Shallow crustal exploration, for mining, geothermal, and sedimentary basin studies, utilizes the frequency range from 1 Hz to 10 kHz while deep crustal exploration utilizes the frequency range from D.C. to 10^2 Hz. The mean slope of the spectrum below 1 Hz is often assumed to be according to f^{-1} whereas we have observed it as high as f^{-4}. The slope of the spectrum is a key to estimates of ratios of signal to noise at frequencies below 0.1 Hz as Connerney et al (1980) have mentioned.

Figure 3 contains natural magnetic field spectra below 3 Hz obtained in recent years in Utah and in Texas, U.S.A. Near 0.1 Hz the spectrum rises with

decreasing frequency in the range of f^{-3} to f^{-4}. SanFilipo and Hohmann (1982) approximate the field data of Figure 3 by assuming that random white noise below 3 Hz was *colored* by a digital filter with a spectral profile indicated by the crosses in this figure. Most people choose to pre-whiten data, via analog filters immediately following the receivers, in order to remove the spectral color. Rather than a conventional pre-whitening, SanFilipo and Hohmann (1982) chose, for simplicity and convenience, a digital high-pass filter to suppress the lower frequencies. The amplitude characteristics of this filter are illustrated in Figure 4. Its characteristics would approximate a conventional analog pre-whitening filter.

Figure 5 illustrates the effect of stacking, alone, and of high-pass filtering plus stacking, of 0.3 Hz magnetic field signal contaminated by the colored noise of Figure 4. The magnetic field is that from a one turn square coil, 1 km to the side, in which a current of 10 amperes exists. The field is measured at a distance of 10 km from the center of the coil. The error bars at 64 and 100 stacks indicate the ensemble standard deviation; the running average correlation output wanders in and out of the expected error range during stacking. It is clear from Figure 5 that many more than 100 stacks are necessary to reduce the noise to an acceptable level if only stacking is used. On the other hand, if the data processing involves high-pass filtering followed by stacking, then a large improvement in signal-to-noise ratio is achieved with far fewer stacks.

By contrast, the high-pass filter offers virtually no improvement at 0.03 Hz as Figure 6 depicts because the noise power within the correlation pass band increases. This would not be true for white noise input where output noise decreases with increasing correlation period, because the data window

length increases. SanFilipo and Hohmann (1982) conclude that, for the transmitter-receiver configuration employed in their analysis, 0.1 Hz is the lowest practical frequency unless a remote reference is used. Use of a remote reference in magnetotellurics is common (Gamble et al., 1979). Its application can be extended to controlled source methods; the Anaconda Company has used it in resistivity/induced polarization surveys for many years (Halverson, 1977). One assumes that the natural fields, which constitute noise for CSEM, are coherent over the distance between the measuring site and the reference site. Cross-correlation between the measuring and remote sites then permits considerable enhancement of signal-to-noise at the measuring site. Figure 7 shows the major improvements in signal-to-noise using this technique; SanFilipo and Hohmann (1982) conclude that remote reference extends the useful frequency range downward by one decade.

Another interesting way to look at stacking and filtering is displayed in Figure 8 for stacks up to 400. The filtering plus stacking is no better than stacking alone at 0.01 Hz and the stacking reduces the square error in the signal according to $\sqrt{N}$ where N is the number of stacks. For stacking only at 0.3 Hz, the improvement for this colored noise is steeper than $\sqrt{N}$ which applies to white noise. Adding the high-pass filter at 0.3 Hz lowers the noise for all stacks and results in $\sqrt{N}$ improvement appropriate to white noise.

Cultural noise

One finds, as Table 2 indicates, that cultural developments create active and passive noise. Circuits completed through fences, pipelines, power lines, telephone lines, rails, and other conductive cultural structures produce anomalies largely unrelated to subsurface geology. These sources of noise can, in rare instances, be reduced by removing the offensive structure, but,

by and large, they can only be avoided by placing transmitters and receivers well away from them. This is not always possible in areas of concentrated industrialization, and hence important geological problems simply cannot be attacked in such areas.

Some of these cultural developments also serve as sources for narrow or broad-band electric and magnetic field noise, especially power lines, telephone lines, and electrified rails as Table 2 indicates. Further compounding the problem is the fact that these active sources of cultural noise induce eddy current noise in the passive cultural noise sources such as fences and pipelines.

Geological noise due to overburden

Overburden can be described variously as unconsolidated sediments, weathered rock, or both; Figure 1 differentiates the two from a geological basis. The overburden may be resistive (e.g., glacial gravels) or conductive (e.g., unconsolidated valley fill in the Great Basin of the U.S.A.). In glaciated terrane both the overburden and the weathered layer may be totally removed as is typical of areas of extensive Precambrian exposure in North America and Scandinavia. The weathered rock is invariably conductive because the geological process of weathering leads to a) increased porosity, b) increased presence of clay minerals with their attendant surficial electrical conduction, and c) increased concentrations of ions in the pore waters of the weathered rocks. In dry climatic environments, evaporation strongly increases the concentration of ions in the pore waters, on average. Dilution of these ions takes place during the rainy season in dry or wet environments. A worldwide study of these factors points out that the shallow resistivity profile is closely related to local climatology, to glaciation, and to

tectonic style. The depth of overburden related to weathering seldom exceeds 100 m but can easily reach 2 km for valley fill in the Great Basin of the U.S.A.

Sedimentary rocks in such areas as the Gulf Coast oil-producing region of Texas and Louisiana in the U.S.A commonly exhibit resistivities as low as 1 to 10 Ω m due to interstitial brines (Pirson, 1963). This also is true of some geothermal areas such as the Imperial Valley in California, U.S.A. (Meidav and Furgerson, 1972) and of deep valley fill containing evaporites in Nevada and Utah, U.S.A. (Ward and Sill, 1976). Values as low as 0.1 Ω m have been recorded in some of these areas. In a broader context than used herein so far, these conductive sediments also can be treated as overburden if one is attempting to study the electrical properties of the deep crust and upper mantle. If a surficial conductive horizon, i.e., overburden of any sort, overlies a substratum to be studied with CSEM, the percent of current entering the substratum becomes of utmost importance. Figure 9 illustrates the fraction of current $f(\alpha)$ confined to the overburden as a function of $\alpha = \frac{2S\rho}{L}$, where S is the conductivity-thickness product of the overburden, ρ is the resistivity of the basement, and L is the distance between the current electrodes (Edwards and Howell, 1976). In order to assure that, say, 80% of the current persists below the overburden, then α must be about 0.3. If the overburden is 1 km thick of resistivity 10 Ω m and the resistivity of the bedrock is 10^3 Ω m, not unreasonable numbers in areas of thick conductive overburden, then the distance between current electrodes needs to be 1000 km to assure that 80% of the current flows in the bedrock. This is an incredible requirement which clearly demonstrates the difficulty of electrically detecting geological structure beneath conductive overburden when using bipolar electric sources. While the analysis has been made for D.C., it

cannot be improved by using A.C. in grounded sources.

When horizontal coil sources are used, induction in the overburden is strictly controlled by θ_1, the induction number of the overburden. This induction number can be decreased by lowering the angular frequency. For example, given an overburden of 1 km thickness and 10 Ω m resistivity excited by an inductive coil source with measurements made at 3×10^{-2} Hz at a distance of 10 km from the source, the value of θ_1 is 0.2, well below values resulting in significant overburden response (Wait, 1955). For MT, the situation is probably better because the skin depth for the same earth model given by

$$\delta = 500 \sqrt{\rho/f} \quad , \qquad (2)$$

is 15 km and thus implies that the 1 km thick overburden of resistivity 10 Ω m is virtually transparent to plane electromagnetic waves of frequency 3×10^{-2} Hz.

From the above we would conclude that the order of preference for sources to be used in regions of high surficial conductivity is a) plane waves, b) inductive coils, and c) grounded bipoles. This is, of course, only a partial analysis of the problem, but it does present the nature of the difficulties of probing the crust and mantle in regions of thick conductive overburden or sediments. Geometrical decay of fields from the three source types, and the attenuation of electromagnetic waves from each of the source types are other factors to consider (Hohmann and Ward, 1981).

Resolution and the effect of other geological noise

To facilitate vertical resolution, i.e., resolution of the resistivities and thicknesses of horizontally layered media, an inductive electromagnetic

system would need to sample at three or four frequencies per decade. At least four decades of spectrum are required if one wishes to explore both shallow and deep layers. If lateral inhomogeneities are superimposed on the layering, then an adequate spatial density of receiving stations must also be assured over a distance sufficiently large to permit delineation of all inhomogeneities of interest. A broad spectrum is necessary if the θ_i of the inhomogeneities cannot be predicted in advance. Data is then best plotted as contours of field quantities in frequency-distance space. We shall illustrate this in discussion of the CSAMT method below.

Roving two-loop sources, to be described subsequently, provide the best lateral resolution. However, for deep crustal/upper mantle electrical exploration we are obliged to use a fixed transmitter, either a loop, a grounded bipole, or a Schlumberger array, and so we are also obliged to accept the lateral resolution that is achievable with these sources.

With a Schlumberger array, frequency is not a variable. Hence increased depth of exploration is achieved through increased current electrode (AB) separation. Lateral inhomogeneities within the array will distort the picture of layering achieved with this array. Hence it is customary to use many overlapping Schlumberger arrays if both vertical and lateral resolution are required. This is referred to as combined sounding-profiling. The dipole-dipole resistivity array is very efficient for combined sounding-profiling.

It is well known that inductive techniques, passive or active, usually provide information on conductivity-thickness products of conductive layers, whereas they usually provide only thickness information on resistive layers. On the contrary, resistivity techniques usually provide information on resistivity-thickness products for resistive layers and conductivity-thickness

products for conductive layers. Vertical resolution of resistive and conductive layers is well illustrated via inversion (e.g., Fullagar and Oldenburg, 1982). Joint inversion of inductive and resistive data sets can markedly improve the resolution (Petrick et al., 1977).

Effects of topography

Table 3 lists three effects of topography on measurements made with an inductive electromagnetic method. Variations in elevation of the receiver relative to the transmitter will produce elevation errors in electric or magnetic fields along a traverse, relative to the fields that would be observed over a flat surface. These can be severe for short separations between transmitter and receiver as might arise in mining and geothermal exploration, but they are not expected to be large for the large separations associated with sedimentary basin or deep crustal/upper mantle studies.

If topographic relief is large, one seeks to assure that a square coil or bipole source is horizontal and that measurements are made of horizontal and vertical magnetic and horizontal electric fields. Alternatively, the plane of the transmitting coil must contain the axis or the plane of the receiving coil and orthogonal magnetic field components are measured relative to this axis or plane. If either one of these alternatives is ignored, *alignment* errors will result.

If, for example, a transmitter is located below and adjacent to a ridge, *induced currents* will occur in the ridge at the higher frequencies and will contribute a source of noise which may obscure subsurface features.

Current channeling

Current channeling occurs due to discontinuity in electric field and a

consequent charge accumulation at a boundary between media of different resistivities. The normal component of current density J_n is continuous across an interface while, by definition, the resistivity ρ is discontinuous. Hence at an interface between media 1 and 2 we find

$$J_{n1} = \frac{E_{n1}}{\rho_1} = \frac{E_{n2}}{\rho_2} = J_{n2} \quad , \tag{3}$$

forcing E_n to be discontinuous at the interface. If $\rho_1 > \rho_2$ then $E_{n1} > E_{n2}$ in order to satisfy this relation; normal electric fields are larger in the medium of highest resistivity adjacent to the boundary. Therefore, at an interface, dielectric displacement $D = \varepsilon E$ must be discontinuous and the fourth Maxwell equation must be written as $\nabla \cdot D = \rho_s$ where ρ_s is a surface charge accumulation. Thus, since two interfaces bound the sides of a two- or three-dimensional body in a homogeneous exterior, a dipolar charge distribution occurs across the body. When the electric field of this body is added to the inducing electric field, the net result is an electric field distribution that causes the current flow in the external medium to be channeled, or "short-circuited" into the body.

Current channeling is most pronounced for MT where plane waves are involved. It becomes of increasing importance at lower frequencies (Wannamaker et al 1982). The phenomenon becomes less as the size of the transmitting source decreases. If the receiver is restricted to regions close to the transmitter, the θ_i referred to earlier may be so small that the system may not observe the current channeling. For a one-, two-, or three-dimensional source, current channeling may occur along one or all axes of the body, depending upon the direction of propagation of the plane wavelets associated with the source. Finally, currents can be channeled from regions exceptionally remote from the body, especially for plane wave excitation.

Depth of exploration

A rule of thumb employed by most geophysicists for a massive sulfide orebody, the principal target for inductive electromagnetic methods applied to mining exploration, is that the depth of exploration is from 0.3 to 1.0 times the separation between transmitting and receiving coils.

If one scales these parameters to deep crustal/upper mantle exploration, the separation between transmitter and receiver would need to be 20 to 60 km for exploration to 20 km. These are numbers totally consistent with those used by Connerney et al. (1980) in deep crustal studies using a horizontal current loop source. Depth of exploration is mostly controlled by target response, geological noise, and separation between transmitter and receiver (Hohmann and Ward, 1981).

Lack of interpretational aids

Undoubtedly the greatest hindrance to application of CSEM is the lack of interpretational aids. One cannot stress too much the need for cost-effective analytic or numerical solutions and catalogs to problems involving plane waves over two-dimensional structures (2D) and three-dimensional structures (3D), three-dimensional sources over two-dimensional structures (2D-3D), and three-dimensional sources over three-dimensional structures (3D-3D). Since Hohmann (this volume) treats this problem in detail, I shall not dwell on it here.

BASIS FOR SELECTING INDUCTIVE ELECTROMAGNETIC SYSTEMS

Time domain, frequency domain, and decades of spectrum

Table 4 itemizes factors to consider in selecting controlled source electromagnetic systems; resistivity and induced polarization methods are not covered by this table but will be treated later. Figures 10 and 11 illustrate the wave forms most commonly used with frequency domain (FEM) and time domain (TEM) electromagnetic systems. Time domain (TEM) systems are much in vogue today in shallow crustal exploration, especially mining and sedimentary basin exploration, because measurements over a broad spectrum may be made in a short period of time whereas FEM systems require much more field time. Further, there is at present an inherently higher sensitivity in TEM than in FEM because TEM measurements are made in the absence of the primary field. On the other hand, power is concentrated in a narrow bandwidth with FEM while it is spread over a broad bandwidth with TEM. Higher ratio of signal to noise results with FEM. This can be countered in TEM if a square wave of low duty cycle is used; it provides short on time and long off time with high instantaneous power. Finally,most commercial state-of-the-art TEM systems operate over two decades of spectrum whereas the few state-of-the-art FEM systems operate over four decades of spectrum. The importance of the use of a large number of decades of spectrum is illustrated in our previous discussions of resolution and geologic noise. If exploration to great depths is desired, then measurements must be made at long times after cutoff of the transmitter current. The noise problems of the FEM methods described earlier apply equally to TEM if one simply replaces "low frequencies" by "long times after current cutoff."

For deep crustal/upper mantle exploration, one might expect that FEM would be favored over TEM because of higher ratio of signal to noise expected

with narrow band (FEM) than with broadband (TEM) systems. While SanFilipo and Hohmann (1982) confirm this notion, further study of the problem is necessary, especially since the signals received from the subsurface targets are model-specific.

Table 5 summarizes the known relative advantages of FEM versus TEM. Apart from these, one should note that a single coil can be used as both transmitter and receiver in TEM. This fact has not yet been exploited in deep crustal/upper mantle exploration, but it is a feature of SIROTEM which has been used in mining and sedimentary basin exploration. Further, alignment errors between transmitter (Tx) and receiver (Rx) are unimportant in TEM because measurement is made only of secondary (scattered) fields whereas in FEM measurements are always made of primary (source) and secondary fields combined.

One can depart from the basic waveforms of Figures 10 and 11 to achieve specific objectives. Duncan et al. (1980) and others report on use of a pseudorandom binary sequence (PRBS) but have yet to demonstrate that this modestly broadband system enjoys advantages over FEM narrow-band systems which also employ cross-correlation to extract signal from noise. Several other waveforms have been used in mining exploration (e.g., Barringer, 1962; Lamontagne, 1975; Won, 1980).

Ratio of signal to noise

Reference to this problem has been made several times above and is noted in Table 4. Insofar as the signal is model-specific and a comprehensive study of model responses remains to be completed, few comments can be made concerning inductive electromagnetic systems. Large transmitter moments, adequate signal processing, and transmitter-receiver configurations which

couple best with the target of interest must be considered. A major deficiency in our knowledge clearly is evident here.

Lateral and vertical resolution

We have earlier drawn attention to lateral and vertical resolution. This sort of an approach has not been documented in CSEM applied to deep crustal/upper mantle exploration but has been documented in AMT/MT applied to the same problem (e.g., Wannamaker et al., 1980). Lateral resolution is important for exploration to depths up to 5 km whereafter vertical resolution is apt to become more important.

Source configurations

Figure 12 portrays four basic transmitting source configurations used in mining exploration. For detailed discussions of the many variants on these basic source types, see Grant and West (1965), Ward (1967), and Telford et al. (1976).

The two-loop array (Figure 12a) is moved in-line or broadside across the expected strike of the structure. In the frequency domain, real and imaginary parts of secondary magnetic fields are recorded as a percentage of primary field. The phase reference is hard-wired from the transmitter to the receiver by which means the primary field is also bucked out. In the time domain, the secondary transient is simply recorded and stacked at the receiver. Measurements are made every 25 or 50 m along traverse with the transmitter and receiver separated by 100 to 200 m.

The large source loop portrayed in Figure 12b ranges in dimensions from 200 m x 400 m to 500 m x 1000 m. Measurements in the frequency domain are made of field strength and phase of one to three magnetic field components or

of field strength ratio and phase difference with a pair of horizontal coplanar or vertical coaxial coils. For the former, synchronized crystal clocks at the receiver and transmitter provide a phase reference for coherent detection. Measurements of one to three components are also made in the time domain for which crystal clocks provide time reference for stacking. Traverses of the receiving coils are made outside the loop on lines perpendicular to a long side of the loop, and hence nominally perpendicular to geologic strike. In the time domain, measurements are also made inside the loop when one wishes to minimize current channeling (pers. comm. B. Spies, 1982). Typical reading intervals are 25 m to 50 m. If two receiving coils are used, they are separated by about 50 m. A scaled-up version of this system suitable for deep crustal studies is represented by the experiments reported by Connerney et al. (1980).

In the time domain it is possible to use a single loop, first as a transmitter and then as a receiver (Figure 12c). Fast switching of the loop from the transmitter to the receiver facilitates this approach. The loop is moved along traverse normal to geologic strike, between measurements, with receiving stations being occupied every 50 or 100 m. The loop typically ranges from 50 m to 100 m to the side. The method is also used in shallow sedimentary basin applications.

The fourth transmitting source shown in Figure 12d is a grounded bipole. As used in the controlled source audiomagnetotelluric method (CSAMT) the bipole is typically 1 to 2 km in length. Readings are made over the frequency range 10 Hz to 10 kHz of components of electric and magnetic fields parallel and perpendicular to the bipole and also of the vertical magnetic field. If measurements are made 3 to 5 skin depths away from the source,

plane wave formulation can be used in interpretation (Skin depths are calculated for the most resistive medium). The bipole is oriented parallel to strike to excite the TE mode whereas it is oriented perpendicular to strike to excite the TM mode. The method is showing recent increased use with applications in mining, geothermal, and sedimentary basins; the measurement station intervals depend upon the scale of the problem (Goldstein and Strangway, 1975; Sandberg and Hohmann, 1980; Bartel and Wayland, 1981). Obviously, the grounded bipole studies of Sternberg (1979) and of Duncan et al. (1980) can be considered related to CSAMT, but their measurements were made closer to the grounded bipole than is typical with CSAMT.

Figures 13 and 14 show, respectively, TM mode field data and TM mode modeled data for a CSAMT survey over the Roosevelt Hot Springs geothermal resource in Utah, U.S.A. Figure 15 contains a) the model that fits the CSAMT TM mode field data, and b) the model that fits a dipole-dipole resistivity survey over the same area. The CSAMT field and model data are from Sandberg and Hohmann (1980) whereas the model derived from the dipole-dipole data is from Ward and Sill (1976). While the earth models derived from the two surveys are somewhat dissimilar, their main features are in consonance. Of importance to detailed deep crustal/upper mantle studies is the fact that the high density of sampling of both spatial and frequency variables does permit an exceptionally high degree of forward fitting of field data. One should not be lulled into believing that all of the parameters of all of the two-dimensional models of Figure 15 have been resolved. Rather these are, while detailed, reasonably permissive models.

One of the least studied matters with inductive CSEM is systematic and objective comparison of the wide range of transmitting and receiving coil

pairs which may be used in exploration for various targets. The reasons for this are the incredible size of the task and the lack of availability of all of the computational methods required to make the comparisons.

For deep crustal/upper mantle exploration the selection of systems becomes considerably simplified relative to the options for mining exploration, for example. To start with, the source most likely will be either a grounded bipole or a square coil. Once one has gone to the considerable logistical trouble of laying out the source, it makes most sense to collect all three orthogonal components of magnetic field and the two horizontal orthogonal components of electric field. However costs, logistics, and objectives may dictate otherwise. The long grounded transmission line is a bipole source. Van Zijl (1977) used long grounded power lines and telephone lines for Schlumberger sounding in a unique display of ingenuity. However, a large single loop, serving first as transmitter and sequentially as receiver, has not been used for such studies as noted earlier. An objective comparative analysis of the advantages and limitations of each of these sources and of MT/AMT in various one-, two-, and three-dimensional terranes is a highly desirable objective for future analysis.

Transmitter source size

Lajoie and West (1976) have demonstrated that the size of the source can be matched to the size of the target in order to achieve optimum response. They conclude that the source dimensions ought to be of the order of the target dimensions if the target is a three-dimensional body.

Other factors

The importance of depth of exploration, current channeling, and effects of topography have been adequately treated under "Problems with inductive CSEM systems" above.

RESISTIVITY AND INDUCED POLARIZATION METHODS

Overview

In Table 6 we list the factors entering into selection of arrays for application of resistivity and induced polarization methods. The factors to consider with these two complementary methods are basically the same as those encountered with the inductive electromagnetic methods with which we have been primarily concerned to this point. However, two different problems arise with resistivity and induced polarization methods, relative to inductive electromagnetic methods. These are discussed in the following.

Array selection

Table 7 lists some factors to consider, and a qualitative evaluation of them, for three different resistivity arrays. Where 1 is entered in a box it indicates the preferred array; where 3 is entered in a box it indicates the least desired array, for that particular factor.

Electromagnetic coupling

The resistivity and induced polarization methods typically use D.C. formulation which requires that the transmitter and receiver are only coupled resistively. However, when A.C. is used, which is customary, then electromagnetic coupling between the transmitter and receiver also occurs. This is readily seen in the expression for mutual coupling between a pair of grounded wires (Sunde, 1949).

$$Z = \int_a^b \int_A^B P(r) \cos\theta + \frac{d^2}{dsdS} Q(r)\, dsdS \,, \qquad (4)$$

in which

$$Q(r) = \frac{1}{2\pi\sigma r} \text{ is the resistive coupling term,} \qquad (5)$$

and

$$P(r) = -\frac{1}{2\pi\sigma r}\left[\frac{1 - (1 + ikr)e^{-ikr}}{r^2}\right] \qquad (6)$$

is the electromagnetic coupling term. The quantities appearing in these relations are: r is the distance between the electrodes a, b, A,B which terminate the wires, θ is the angle between the wires, σ is the conductivity of the half-space upon which the wires are situated, $k = (-i\ \sigma\ \mu\omega)^{1/2}$ is the wavenumber of the half-space, μ is the permeability of the half-space, and ω is angular frequency.

The electromagnetic coupling between the wires increases with frequency, with the lengths ab and AB, with the separation between ab and AB, and with the conductivity of the half-space. As Table 7 indicates, the dipole-dipole array is superior to the Schlumberger array in this respect. Van Zijl (1977) avoided electromagnetic coupling in his long-line Schlumberger sounding by waiting until all transients died away before making a measurement; this is the normal procedure when operating in the time domain. When operating in the frequency domain, sufficiently low frequencies are used to eliminate the problem. Electromagnetic coupling is particularly important to the induced polarization method where one is attempting to measure resistivity as a slowly varying function of frequency, the latter due to electrochemical reactions in the subsurface. As can be seen from the formulation above, electromagnetic coupling is also frequency dependent and it can totally obscure the induced polarization effects. Moreover, for deep crustal studies, values obtained in a resistivity survey can be grossly in error if D.C. formulation is used. Hence the full A.C. formulation should be used in those areas and with those techniques that demand it.

Lateral effects

The depths of exploration of three resistivity arrays are given by Roy and Apparao (1971) for Schlumberger as 0.125L, and for dipole-dipole as 0.195L, where L is the maximum separation between extreme electrodes (AB for Schlumberger). Thus Schlumberger uses 1.6 times the maximum electrode separation as the dipole-dipole method for the same depth of exploration. This makes it more susceptible to the effects of inhomogeneities offset from the sounding. On the other hand it is well known (e.g., Kunetz, 1966) that the Schlumberger array is least affected by near-surface inhomogeneities beneath the array.

DEEP CRUSTAL APPLICATIONS

Some recent deep crustal CSEM studies

Table 8 summarizes the results of five recent CSEM field experiments. Two experiments used grounded dipole sources of about 20 km length, one used a grounded power line of 1400 km length, one used power and telephone lines in numerous Schlumberger arrays, while one used a loop source of 4.5 km diameter. The other pertinent details of the experiments are included in Table 8. Even the most casual inspection of Table 8 will reveal that these deep crustal studies are logistically difficult. Lienert and Bennett (1977) performed their sounding in the western Basin and Range Province, U.S.A.; Sternberg (1979) performed his in Precambrian terrane of Wisconsin, U.S.A.; Connerney et al. (1980) worked in the Precambrian of the Adirondack Mountains, U.S.A.; Duncan et al. (1980) made measurements in the Precambrian of eastern Canada; while Van Zijl (1977) made his measurements in the Precambrian of southern Africa. Each of the five experiments detected a conductive (10 to 1000 Ωm) layer in the deep crust at depths varying from about 20 to 40 km.

The most widely accepted cause for such low resistivity at such great depths is hydrated mantle rock in the form of serpentinite. Is this due to the abundance of platey minerals which exhibit large mineral surface conduction effects (Ward and Fraser, 1967)? There is not a definitive explanation for this conduction mechanism at this time.

G. R. Olhoeft (pers. comm., 1982) confirms that serpentine at 500°C and riebeckite (an amphibole) at 400°C can exhibit resistivities as low as 10 Ω m. Stesky and Brace (1973) note that serpentine with abundant magnetite, as is common, exhibits resistivities less than 10 Ω m at 6 kbar (15 to 20 km) due to electrical contact between the magnetic mineral grains. The presence of

hydrated minerals in the lower crust in sufficient quantities to form a widespread interconnected phase, while appealing in that it would satisfy both electrical and seismic anomalies at 15 to 25 km depths, is debatable (Connerney et al., 1980).

The notion of conducting mineral grains in contact to form a low resistivity network, as found by Stesky and Brace (1973) provides stimulus for finding conducting minerals, other than magnetite, to serve this purpose. Graphite is abundant in Archean rocks, especially schists (e.g. Nash, Granger, and Adams, 1981). If the film of graphite was sufficiently thin and was connected around all silicate mineral grains, less than 1% graphite would be sufficient (Olhoeft, pers. comm., 1982). Partial melting in the lower crust is the explanation preferred by Lienert and Bennett (1977) for low resistivities in the northwestern Basin and Range Province in the U.S.A.

One might question the assumption of an infinite line source and the ignoring of near-surface geologic noise in the experiment performed by Lienert and Bennett (1977). Duncan et al. (1980) admitted that lateral variations in resistivity were probably affecting their interpretations. Van Zijl (1977) performed numerous detailed Schlumberger arrays in order to assess the effects of lateral inhomogeneities. Connerney et al. (1980) and Sternberg (1979) seemed to have found locations largely devoid of lateral inhomogeneities.

An experiment with dipole-dipole sounding - profiling in the eastern Basin and Range Province, Utah, USA

Several years ago we experimented with crustal exploration using the dipole-dipole array. The site we chose was near a high-temperature geothermal resource located at Roosevelt Hot Springs near Milford, Utah. Figure 16 shows the pseudosection resulting from this survey. Both 3 km and 6 km dipoles were

used and resulted in, according to Roy and Apparao (1971), depths of exploration of 3 km and 6 km respectively. However, when the 3 km data were inverted to three or five alpha centers, the locations of the alpha centers (Figure 17) were only reliably estimated at depths of much less than 1 km (Petrick et al, 1981). The near-surface resistivity inhomogeneities precluded exploration to depths predicted on the basis of a plane-layered earth model. We shall explore further the influence of near-surface inhomogeneities in subsequent discussion.

Deep crustal exploration in the eastern Basin and Range Province, Utah, USA

The Basin and Range Province is characterized by NNE-trending mountain ranges and deep sediment-filled valleys. Regional lithospheric extension commencing about 20 m.y. ago yielded the elongate uplifted mountain blocks bounded by normal faults. Subsequent erosion filled the intervening valleys with conductive sediments commonly as deep as 2 km. The mountains, in contrast, are electrically resistive. Performing electrical exploration of the deep crust and upper mantle beneath this surficially complex geoelectric section requires the use of two- and three-dimensional numerical modeling algorithms.

In 1976, 1977, and 1978 we carried out extensive magnetotelluric soundings in an area of the eastern Basin and Range near Milford, Utah (Wannamaker et al, 1980). Although the geoelectric section in the top 2 km was clearly three-dimensional, we approximated it by two-dimensional models since the mountain and valley involved in our studies were quite elongate. However, we restricted our interpretations to the TM mode of excitation (or E perpendicular to the axes of mountain and valley) since it is the only 2D mode that includes current channeling. In Figure 18 we show the model of the

subsurface which provides the best fit of TM mode MT observations at each of the 13 stations shown in the figure. Both the apparent resistivity and impedance phase were computed over the frequency range 10^{-3} Hz to 10^{2} Hz.

The pseudosections of apparent resistivity and impedance phase calculated for the model of Figure 18 were almost identical to the observed pseudosections as comparison of Figures 19 and 20 will attest. While not all of the parameters of all of the blocks above 2 km are necessarily well resolved, nevertheless all of the blocks were required to produce the excellent fit between computed and observed pseudosections.

Below 2 km, only plane horizontal layering was included in the geoelectric section since the lower frequency portions of the MT data sets were all virtually identical. In Figure 21, we show the vertical resistivity profile from 2 km to 85 km, reflecting the plane-layered nature of the crust and mantle over that interval. From surface to about 15 km the conduction is via water-filled pores, fractures, and faults. From 15 km to 35 km semiconduction dominates, while from 35 km to 65 km the extremely low resistivity can only be accounted for by partial melt (Wannamaker et al., 1980). Only by use of a high spatial density of stations and a broad bandwidth were we able to delineate both the shallow and the deep electrical structures. We would prefer frequencies as low as 10^{-4} Hz for deeper probing and frequencies as high as 10^{4} Hz for better delineation of the near surface inhomogeneities. Unless the latter are well delineated, modeling of the layering beneath them becomes uncertain. Fortunately we had shallow dipole-dipole resistivity, in this instance, to help us achieve the model of Figure 18. If one uses the range 10^{-4} Hz to 10^{4} Hz, the method should be referred to as MT/AMT.

With this model of the crust and mantle now in hand we would very much like to verify it by use of CSEM. Also, we would like to attempt to use joint inversion of the MT and CSEM data (e.g., Petrick et al., 1977) to achieve greater parameter resolution. The principal question which then immediately arises is: "can we model the inhomogeneous top 2 km of the geoelectric section so as to reveal the layering in the deep crust and upper mantle?" The next question to ask is: "can we get enough field strength from a practical grounded bipole or loop source to permit energizing the deep crust and upper mantle?" In the next two sections we address these two questions.

The effects of three-dimensional deep valley fill on CSEM

The algorithms we use for modeling MT or CSEM with 3D bodies are modifications of an integral equation formulation attributable to Hohmann (1975). They are expensive to utilize for all but the simplest of bodies. Further, the 3D body cannot be at surface if convergence of the numerical approximation is to be at all within time and cost bounds. Still further, they are limited to a resistivity contrast between the 3D body and its surroundings of about 2500:1.

Finally, because of excessive costs, one cannot consider modeling more than one valley and one mountain at a time. This latter constraint forces us to limit the source dimensions to the valley dimensions. From a practical viewpoint one could not lay out a grounded bipole in the mountains due to lack of access. Even if access was not a problem, the source would assume a very irregular shape if it were draped along or across a mountain range. Thus the source must sensibly be kept in the valley or in the low foothills of the mountains. All of the above explains our reasons for selecting the source dimensions and the simple model of conductive valley fill which we shall

discuss next.

Figure 22 shows the simple model of the conductive valley fill; it is 36 km NS, 14 km EW, and 1 km deep and is buried 1 km beneath resistive overburden. It is excited at 0.03 Hz in turn by a 20 km NS grounded bipole, i.e., parallel to the long axis of the valley fill, by a 20 km EW grounded bipole, and by a square loop 5 km to the side. We chose 0.03 Hz as the lowest practical frequency one would attempt to use with these sources since low ratio of signal to noise would virtually prohibit use of lower frequencies. A somewhat larger NS grounded bipole and a somewhat larger square loop would be used for deep crustal/upper mantle exploration, but a larger EW grounded bipole could not sensibly be used because of the mountains. A Schlumberger array is out of the question, for if AB was set equal to 36 km then the depth of exploration would only be 4.5 km. The model we are using is a primitive representation of the valley fill shown in cross section in Figure 18.

Figure 23 shows the amplitude and phase of the total horizontal magnetic (EW) field normalized by the primary field values for the north-south grounded bipole. The amplitude of the horizontal magnetic field over the body rises to more than 3 times the primary field. Off the body it falls to 60% of the primary field. In Figure 24 are plotted the amplitude and phase of the normalized vertical magnetic field. The amplitude of the vertical magnetic field rises to about 130% of the primary field above the valley and drops to 60% of the primary field to the east of the valley. In Figure 25 are plotted the phase and amplitude of the normalized (NS) electric field. Throughout, the amplitude is less than 40% of the primary field.

Channeling of the bipole return current through the valley fill would explain all of the above observations. As far as deep crustal and upper

mantle exploration is concerned, the source looks like a loop and not a bipole. One could calculate whether or not the various layers of Figure 18 could be detected with such a complex source. We have not yet done this. It seems problematical to us that we could model the geoelectric section in full three dimensions to a sufficient degree of precision to permit detecting layering at depths greater than the 2 km depth of the near-surface inhomogeneities. In this example we set the NS bipole 1 km to the east of the valley fill because in Milford Valley a north-south access road occurs in this locality. The bipole could not be moved further east because of the mountains.

Figure 26 portrays the behavior of the amplitude and phase of the normalized east-west horizontal magnetic field for a 5 km by 5 km square loop. The distortions in the horizontal magnetic field are every bit as severe as for the NS grounded bipole. The distortions of the vertical component don't appear so bad, but that is because all secondary fields, including any scattered by a deep layer, are very small compared to the strength of the vertical primary field. One would conclude, as for the bipole source, that adequate removal of the effects of a three-dimensional valley would be problematical. In any event the costs of the modeling would be prohibitive.

Figure 27 exhibits the behavior of the amplitude and phase of the normalized horizontal magnetic field for a 20 km grounded bipole placed across the valley fill model of Figure 22. The distortions are not as bad for this source type as they are for the other two. This probably occurs because the grounds of the bipole were 3 km on either side of the valley. Such a placement is possible in the Milford Valley but the source would have the

appearance of a catenary because of the topographic relief of the sloping valley floor and the mountains. However, the ends would be only 1.5 km above the center of the catenary. This seems to be the most promising source type to use, and since it excites the TM mode primarily, it seems possible that 2D-3D modeling rather than 3D-3D modeling could be used if an algorithm existed for this case. Cost and accuracy improvements are expected with 2D-3D compared to 3D-3D modeling.

Selection of a source for deep crustal/upper mantle exploration

One would certainly elect to use transmission lines and/or telephone lines as Lienert and Bennett (1977) and Van Zijl (1977) have done, if such lines were available. They both afford adequate ratio of signal to noise without excessive stacking. Further, they both explore to upper mantle depths. Without such long line sources, which only occasionally become available, one is then left with MT/AMT, grounded bipole, or loop sources. In terranes where thick irregular conductive materials exist at surface it would appear prudent, from our computations, to use MT/AMT. If the overburden is relatively thin and uniform then a horizontal loop may be preferred according to our earlier analysis. However, if no overburden exists then either a loop source or a grounded bipole source may be used provided their moments are equal and provided ground contacts are not a problem for the bipole source.

In Table 9 we list the minimum characteristics a CSEM system would need for complete crustal sounding and profiling. This system would be used to detect both lateral and vertical variations in resistivity from surface to depths of order 30 to 40 km. The system used by Connerney et al. (1980) meets most of the characteristics listed in Table 9. These authors prewhitened their data but did not describe otherwise the filter characteristics used to

reject low-frequency noise. Their highest frequency was 400 Hz since they did not attempt to map the near surface.

SanFilipo and Hohmann (1982) have established that a remote reference must be placed at a distance of at least 5 times the separation between the receiving and the transmitting sites. Achievement of this remote reference would seem to be impractical when Tx-Rx separations as large as 100 km are required for deep crustal/upper mantle exploration.

One might want to use both a grounded bipole and a loop source and employ joint inversion to improve the resolution of the layered media in the geoelectric section.

CONCLUSIONS

If a CSEM experiment is to deduce the lateral and vertical variation in resistivity to depths on the order of 30 to 40 km, it should be placed to avoid regions of electrification, geological, cultural, and topographic noise. The main problem then met is dealing with natural field noise; a lower frequency limit near 3×10^{-2} Hz probably would be dictated by this noise. While most deep crustal/upper mantle experiments performed so far have concentrated on layered resistivity distributions, experiments of the future should be designed to ensure resolution of both lateral and vertical variations in resistivity from surface to the maximum depth of the experiment.

Controlled source electrical methods offer an advantage over MT/AMT in that they do not suffer nearly as much from current channeling in distant overburden or oceans. On the other hand, frequencies as low as 10^{-4} Hz are readily available for MT and hence deeper exploration is possible with this latter method. Either a grounded bipole or a loop source is satisfactory for deep crustal exploration if a controlled source is warranted. Use of both source types in the same experiment offers the improved resolution of layered models available via joint inversion of the two resulting data sets. CSEM experiments do not seem well suited to delineating deep crustal and upper mantle resistivity distributions in regions where irregular overburden exists; the MT/AMT method is preferred there, because of the availability of 2-D modeling algorithms and because of the availability of ultra-low frequencies.

Five recent experiments each detected a low-resistivity zone in the crust at depths ranging from about 15 to 30 km. The geological explanation most commonly offered for this zone is surficial conduction in serpentinized rocks but other explanations should be sought. Graphite is a logical alternative.

Of the five experiments, four were performed in Precambrian terranes with two using grounded bipoles, one using a loop source, and one using a Schlumberger array via transmission and telephone lines. The fifth experiment was conducted in the western Basin and Range Physiographic Province in the U.S.A. The logistics involved in all five experiments were formidable.

ACKNOWLEDGEMENTS

I wish to thank W. A. SanFilipo and P. E. Wannamaker for computations of the effects of three-dimensional bodies on the fields of finite sources. Further, I wish to thank them and W. R. Petrick for critically reviewing this manuscript. Holly Baker and Joan Pingree typed the manuscript. Sandra Bromley and Doris Cullen supervised the preparation of the illustrations.

Preparation of this manuscript has been made possible by a grant from the Mobil Foundation, Inc.

REFERENCES

Barringer, A. R., 1962, The INPUT electrical pulse prospecting system: Min. Cong. J., v. 48, p. 49-52.

Bartel, L. C., and Wayland, J. R., 1981, Results from using the CSAMT geophysical techniques to map oil recovery processes: Preprint SPE 10230, Soc. of Petroleum Engineers of AIME., 9 p.

Campbell, W. H., 1967, Geomagnetic pulsations, *in* S. Matsushita and W. H. Campbell, eds., Physics of geomagnetic phenomena: New York, Academic Press, p. 822-909.

Connerney, J. E. P., Nekut, A., and Kuckes, A. F., 1980, Deep crustal electrical conductivity in the Adirondacks: J. Geophys. Res., v. 85, p. 2603-2614.

Duncan, P. M., Hwang, A., Edwards, R. N., Bailey, R. C., and Garland, G. D., 1980, The development and applications of a wide band electromagnetic sounding system using a pseudo-noise source: Geophysics, v. 45, p. 1276-1296.

Edwards, R. N., and Howell, E. C., 1976, A field test of the magnetometric resistivity (MMR) method: Geophysics, v. 41, p. 1170-1183.

Fullagar, P. K., and Oldenburg, D. W., 1982, Inversion of horizontal loop electromagnetic soundings: Geophysics, in press.

Gamble, T. D., Goubau, W. M., and Clarke, J., 1979, Magnetotellurics with a remote reference: Geophysics, v. 44, p. 53-68.

Goldstein, M. A., and Strangway, D. W., 1975, Audiofrequency magnetotellurics with a grounded electric dipole source: Geophysics, v. 40, p. 669-683.

Grant, F. S., and West, G. F., 1965, Interpretation theory in applied geophysics: New York, McGraw-Hill Book Company, 583 p.

Halverson, M. O., 1977, I.P. research and development directions, *in* Geophysics applied to detection and delineation of non-energy non-renewable resources: Proc. of Workshop on Mining Geophysics, Dept. Geology and Geophysics, Univ. of Utah.

Hohmann, G. W., 1975, Three-dimensional induced polarization and electromagnetic modeling: Geophysics, v. 40, p. 309-324.

Hohmann, G. W., and Ward, S. H., 1981, Electrical methods in mining geophysics: Economic Geology, 75th Anniversary Volume, p. 806-828.

Kunetz, G., 1966, Principles of direct current resistivity prospecting: Berlin, Gebruder Borntraeger, 103 p.

Lajoie, J. J., and West, G. F., 1976, The electromagnetic response of a conductive inhomogeneity in a layered earth: Geophysics, v. 41, p. 1133-1156.

Lamontagne, Y. L., 1975, Applications of wide-band time domain EM measurements in mineral exploration: Ph.D. thesis, University of Toronto.

Lienert, B. R., and Bennett, D. J., 1977, High electrical conductivities in the lower crust of the northwestern Basin and Range: an application of inverse theory to a controlled-source deep-magnetic-sounding experiment, *in* J. G. Heacock, ed., The Earth's Crust: Am. Geophys. U. Geophysical Monograph 20, p. 531-552.

Meidav, T., and Furgerson, R., 1972, Resistivity studies of the Imperial Valley geothermal area, California: Geothermics, v. 65, p. 47-62.

Mysen, B. O., and Kushiro, I., 1977, Compositional variations of coexisting phases with degree of melting of peridotite in the upper mantle: Am. Min., 62, p. 843-865.

Nash, J. T., Granger, H. C., and Adams, S. S., 1981, Geology and concepts of genesis of important types of uranium deposits *in* B. J. Skinner, ed., Economic Geology 75th Anniversary Volume, p. 63-116.

Petrick, W. R., Pelton, W. H., and Ward, S. H., 1977, Ridge regression inversion applied to crustal resistivity sounding data from South Africa: Geophysics: v. 42, p. 995-1005.

Petrick, W. R., Sill, W. R., and Ward, S. H., 1981, Three-dimensional resistivity inversion using alpha centers: Geophysics, v. 46, p. 1148-1162.

Pirson, S. J., 1963, Handbook of well log analysis: Englewood Cliffs, N.J., Prentice-Hall, Inc., 326 p.

Rai, C. S., and Manghnani, M. H., 1978, Electrical conductivity of basalts to 1550°C, *in* H. J. B. Dick, ed., Proceedings of Chapman Conference on Partial Melting in the Earth's Mantle: Oreg. Dept. Geol. Min. Ind. Bull. 96, p. 219-232.

Roy, A., and Apparao, A., 1971, Depth of investigation in direct current resistivity prospecting: Geophysics, v. 36, p. 943-959.

SanFilipo, W. A., and Hohmann, G. W., 1982, Computer simulation of low-frequency electromagnetic data acquisition: Earth Science Lab., Univ. of Utah Research Institute, report 62, 33 p.

Sandberg, S. K., and Hohmann, G. W., 1980, Controlled-source audiomagnetotellurics in geothermal exploration: Geophysics, v. 47, p. 100-116.

Scarfe, C. M., Mysen, B. O., and Rai, C. S., 1978, Invariant melting of mantle material: partial melting of two lherzolite nodules: Yearbook of the Carnegie Inst. of Washington, 78, p. 498-501.

Sternberg, B. K., 1979, Electrical resistivity structure of the crust in the southern extensions of the Canadian Shield-layered earth models: Jour. Geophys. Res., v. 84, p. 212-228.

Stesky, R. M., and Brace, W. F., 1973, Electrical conductivity of serpentinized rocks to 6 kbars: Jour. Geophys. Res., v. 78, p. 7614-7621.

Sunde, E. D., 1949, Earth conduction effects in transmission systems: New York, D. Van Nostrand Co., Inc., 373 p.

Telford, W. M., Geldart, L. P., Sherrif, R. E., and Keys, D. A., 1976, Applied geophysics: London, Cambridge Univ. Press, 860 p.

Van Zijl, J. S. V., 1977, Electrical studies of the deep crust in various tectonic provinces of southern Africa, *in* The Earth's Crust, J. G. Heacock, ed., Am. Geophys. U. Geophysical Monograph 20, p. 470-500.

Vaughn, P. J., and Kohlstedt, D. L., 1980a, Solid-melt structure in a partially melted olivene basalt mixture: EOS Transactions, 61(17), p. 396.

Vaughn, P. J., and Kohlstedt, D. L., 1980b, Effect of degree of textural equilibrum on melt distribution in olivene-basalt mixtures: EOS Transactions, 61(46), p. 1132.

Waff, H. S., and Bulau, J. R., 1979, Equilibrium fluid distribution in an ultramafic partial melt under hydrostatic stress conditions: J. Geophys. Res., 84 (B11), p. 6109-6114.

Wait, J. R., 1955, Mutual electromagnetic coupling of loops over a homogeneous ground: Geophysics, v. 20, p. 630-637.

Wannamaker, P. E., Ward, S. H., Hohmann, G. W., and Sill, W. R., 1980, Magnetotelluric models of the Roosevelt Hot Springs Thermal Area, Utah: Dept. Geology and Geophysics, Univ. of Utah, report 27002-8, 313 p.

Wannamaker, P. E., Ward, S. H., and Hohmann, G. W., 1982, Magnetotelluric responses of three-dimensional bodies in layered earths: Earth Science Lab., Univ. Utah Research Institute, in press.

Ward, S. H., 1967, The electromagnetic method, *in* Mining Geophysics Vol. II: Tulsa, Soc. of Exploration Geophysicists, p. 224-372.

Ward, S. H., and Fraser, D. C., 1967, Conduction of electricity in rocks, *in* Mining Geophysics Vol. II.: Tulsa, Soc. Exploration Geophysicists, p. 197-223.

Ward, S. H., and Sill, W. R., 1976, Dipole-dipole resistivity surveys, Roosevelt Hot Springs KGRA: NSF final report, N.S.F. Grant GI-43741, Dept. Geol. Geophys., Univ. of Utah, 29 p.

Won, I. J., 1980, A wide-band electromagnetic exploration method - Some theoretical and experimental results: Geophysics, v. 45, p. 928-940.

Wyllie, P. H., 1979, Petrogenesis and the physics of the earth, *in* H. S. Yoder, Jr., ed., The evolution of the igneous rocks: Fiftieth Anniversary Perspectives: Princeton Univ. Press, p. 483-520.

LIST OF TABLES

PROBLEMS WITH E.M.

- NATURAL FIELD NOISE
- CULTURAL NOISE
- EFFECT OF OVERBURDEN
- EFFECT OF OTHER GEOLOGIC NOISE
- EFFECT OF TOPOGRAPHY
- RESOLUTION
- CURRENT CHANNELING
- NEED FOR MORE 2D, 2D-3D, AND 3D ALGORITHMS

CULTURAL NOISE

⇨PASSIVE

- FENCES
- PIPELINES
- POWER LINES
- TELEPHONE LINES
- RAILS

⇨ACTIVE

- POWER LINES
- TELEPHONE LINES
- ELECTRIFIED RAILS

EFFECTS OF TOPOGRAPHY

- ELEVATION ERRORS
- ALIGNMENT ERRORS
- CURRENT CHANNELING IN RIDGES

BASIS FOR SELECTING CSEM SYSTEMS

- TEM OR FEM
- DECADES OF SPECTRUM
- S/N RATIO
- LATERAL & VERTICAL RESOLUTION
- SOURCE CONFIGURATION
- Tx COIL SIZE
- DEPTH OF EXPLORATION
- CURRENT CHANNELING
- EFFECTS OF TOPOGRAPHY

FEM VS TEM				
	SPECTRUM	BANDWIDTH	Tx-Rx SEPARATIONS	ALIGNMENT ERRORS
F.D.	4 Decades	Narrow	Large	Problem
T.D.	2 Decades	Broad	Small	No Problem

	TIME/READING	SIGNAL	NOISE	INSTANTANEOUS POWER
F.D.	Large	Model Specific	Low	Low
T.D.	Small	Model Specific	High	High

BASIS FOR SELECTING ρ_a/IP ARRAYS

- TD OR FD
- DECADES OF SPECTRUM
- S/N RATIO
- LATERAL & VERTICAL RESOLUTION
- ARRAY SELECTION
- DEPTH OF EXPLORATION
- CURRENT CHANNELING
- EFFECTS OF TOPOGRAPHY

RESISTIVITY ARRAY EVALUATION					
	S/N RATIO	LAT. RES.	D. OF E.	LAT. EFF.	EM COUPLING
Schlumberger	1	3	3	3	3
Pole-Dipole	2	2	2	2	2
Dipole-Dipole	3	3	1	1	1

RECENT EXPERIMENTS USING CSEM FOR DEEP CRUSTAL STUDIES

INVESTIGATORS	SOURCE TYPE	SOURCE CURRENT	BANDWIDTH	Tx-Rx SEPARATION	WAVEFORM	STACKING TIME	CRUSTAL MODEL
LIENERT & BENNETT, 1977	1400 km GROUNDED POWER LINE	300A	0.001-0.01 Hz	5-55 km	SQUARE	20 STACKS	0 — 20 10^2-10^3 Ωm 35-45 1-10 Ωm km 100 Ωm
STERNBERG, 1979	22-24 km GROUNDED BIPOLE	70A	0.5-10 Hz	5-40 km	SQUARE	100 STACKS	0 — 10 10^3 Ωm 14-22 10^5 Ωm km 50-1200 Ωm
CONNERNEY, F T AL; 1980	4.5 km DIA. LOOP	65A	0.05-400 Hz	20-65 km	SQUARE	TO DAYS	0 — 10 10^4 Ωm 20 10^3 Ωm 30 10-25 Ωm km 10^4 Ωm
DUNCAN ET AL; 1980	20.5 km GROUNDED BIPOLE	5A	1.0-50 Hz	35-85 km	PRBS	TO 10 HRS	0 — 17-29 1.5×10^4 Ωm km 270 Ωm
VAN ZIJL, 1977	SCHLUMBERGER	72A	D.C.	AB TO 1000 km	SQUARE	174 STACKS	0 — 25-30 $2\text{-}10 \times 10^3$ Ωm 30-40 10-60 Ωm km HIGHLY RESISTIVE

CSEM FOR DEEP CRUSTAL PROBING

- T_x - BIPOLE 20 km LENGTH
  - LOOP 20 km CIRCUMFERENCE
- R_x - E_x, E_y, H_x, H_y, H_z, (H sensor RMS noise $\leq 10^{-4}\gamma$)
- 3×10^{-2} Hz TO 10^4 Hz, 3 TO 4 PER DECADE
- 50 TO 100 AMPS
- 1 TO 100 km, HIGH DENSITY
- 12 BIT A TO D.
- COHERENT DETECTION
- HIGH PASS FILTER PLUS STACKING
- CRYSTAL CLOCK REFERENCE

FIGURE CAPTIONS

Figure 1 The generalized geologic model used for the electromagnetic method in the search for massive sulfides.

Figure 2 Generalized spectrum of natural magnetic fields (After Campbell, 1967).

Figure 3 Amplitude spectral density of geomagnetic noise and matching amplitude spectral density of synthetic noise (After SanFilipo and Hohmann, 1982).

Figure 4 The digital high-pass filter transfer function for data collected at a base frequency f_0 (After SanFilipo and Hohmann, 1982).

Figure 5 A simulation of the running average real component of frequency domain CSEM data acquisition at 0.3 Hz in the presence of natural field noise (After SanFilipo and Hohmann, 1982).

Figure 6 A simulation of the running average real component of frequency domain CSEM data acquisition at 0.03 Hz in the presence of natural field noise (After SanFilipo and Hohmann, 1982).

Figure 7 A simulation of the running average real component of frequency domain CSEM data acquisition at 0.3 Hz using a remote reference for reduction of natural field noise. (After SanFilipo and Hohmann, 1982).

Figure 8 Frequency domain output noise at 0.01 Hz and 0.3 Hz for colored synthetic input noise at various numbers of cycles stacked. σ_Y is the output variance. (After SanFilipo and Hohmann, 1982).

Figure 9 The function $f(\alpha)$ which determines the percentage of current remaining in a conductive, thin surface layer above a resistive half-space (After Edwards and Howell, 1976).

Figure 10 Frequency domain transmitted and received waveforms. Sine wave decomposed into in-phase and quadrature components. Amplitude is designated by A, phase by ϕ, period by T, and frequency by f.

Figure 11 Typical time domain transmitted and received waveforms.

Figure 12 The four basic source types used in electromagnetic exploration: (a) coplanar horizontal, coplanar vertical, or coaxial loop pairs; (b) a large rectangular source loop to which a single horizontal or vertical receiving coil is referenced; (c) a single loop which is used sequentially as transmitter and as receiver in the time domain or whose impedance is measured in the frequency domain; and (d) a grounded wire source to which electric and magnetic field components are referenced.

Figure 13 TM mode CSAMT field data, Roosevelt Hot Springs, Utah, U.S.A. (After Sandberg and Hohmann, 1980).

Figure 14 TM mode CSAMT modeled data, Roosevelt Hot Springs, Utah, U.S.A. (After Sandberg and Hohmann, 1980).

Figure 15 Two-dimensional model from which the modeled data of Figure 19 were calculated (top) and two-dimensional model derived from dipole-dipole resistivity survey (bottom) (After Sandberg and Hohmann, 1980).

Figure 16 Resistivity pseudosection from combined 3 km and 6 km dipole-dipole survey near Roosevelt Hot Springs, Utah, U.S.A.

Figure 17 Dipole-dipole resistivity data and two sets of inversion results illustrating the trade-off between data fit and parameter resolution when more α centers are used in the inverse solution. The plots to the left show the results when only three α centers are used to define the conductivity distribution, while those on the right show the results for five centers. If any deep conductors exist in this region, the α center inversion scheme failed to discriminate between their response and the near-surface conductive areas. The dipole length is 3 km. Data acquired near Roosevelt Hot Springs, Utah, U.S.A. (After Petrick et al., 1981).

Figure 18 2D TM mode finite element section used to compute the modeled apparent resistivity and impedance phase pseudosections of Figure 20. Roosevelt Hot Springs, Utah, U.S.A. (After Wannamaker et al., 1980).

Figure 19 Observed apparent resistivity and impedance phase pseudosections. Contours of resistivity are in Ω m while those of phase are in degrees. Roosevelt Hot Springs, Utah, U.S.A. (After Wannamaker et al., 1980).

Figure 20 Modeled apparent resistivity and impedance phase pseudosections. Contours of resistivity are in Ω m while those of phase are in degrees. Roosevelt Hot Springs, Utah, U.S.A. (After Wannamaker et al., 1980).

Figure 21 Best-fit crust and upper mantle resistivity profile beneath Roosevelt Hot Springs, Utah, U.S.A. (After Wannamaker et al., 1980). The curve of dashes and dots corresponds to bulk resistivity of partially melted peridotite using the melt fraction determinations of Mysen and Kushiro (1977), Scarfe et al. (1978) and Wyllie (1979), the melt phase interconnection model of Waff and Bulau (1979) and Vaughn and Kohlstedt (1980a; 1980b), and the melt phase conductivity measurements on alkali olivene basalts of Rai and Manghnani (1978). Individual numbers on the partial melting curve indicate percentage of liquid phase.

Figure 22 Model used to calculate approximate response of a valley fill to excitation of a NS 20 km grounded bipole (x directed), an EW 20 km grounded bipole (y directed), and a 5 km square loop.

Figure 23 Amplitude and phase of the normalized horizontal magnetic field for the NS grounded bipole adjacent to the valley fill model shown in Figure 29.

Figure 24 Amplitude and phase of the normalized vertical magnetic field for the NS grounded bipole adjacent to the valley fill model shown in Figure 29.

Figure 25 Amplitude and phase of the normalized horizontal electric field for the NS grounded bipole adjacent to the valley fill model shown in Figure 29.

Figure 26 Amplitude and phase of the normalized east-west horizontal magnetic field for the 5 km square loop overlapping the valley fill model shown in Figure 29.

Figure 27 Amplitude and phase of the normalized NS magnetic field for the EW grounded bipole straddling the valley fill model shown in Figure 29.

EM SEARCH PROBLEM

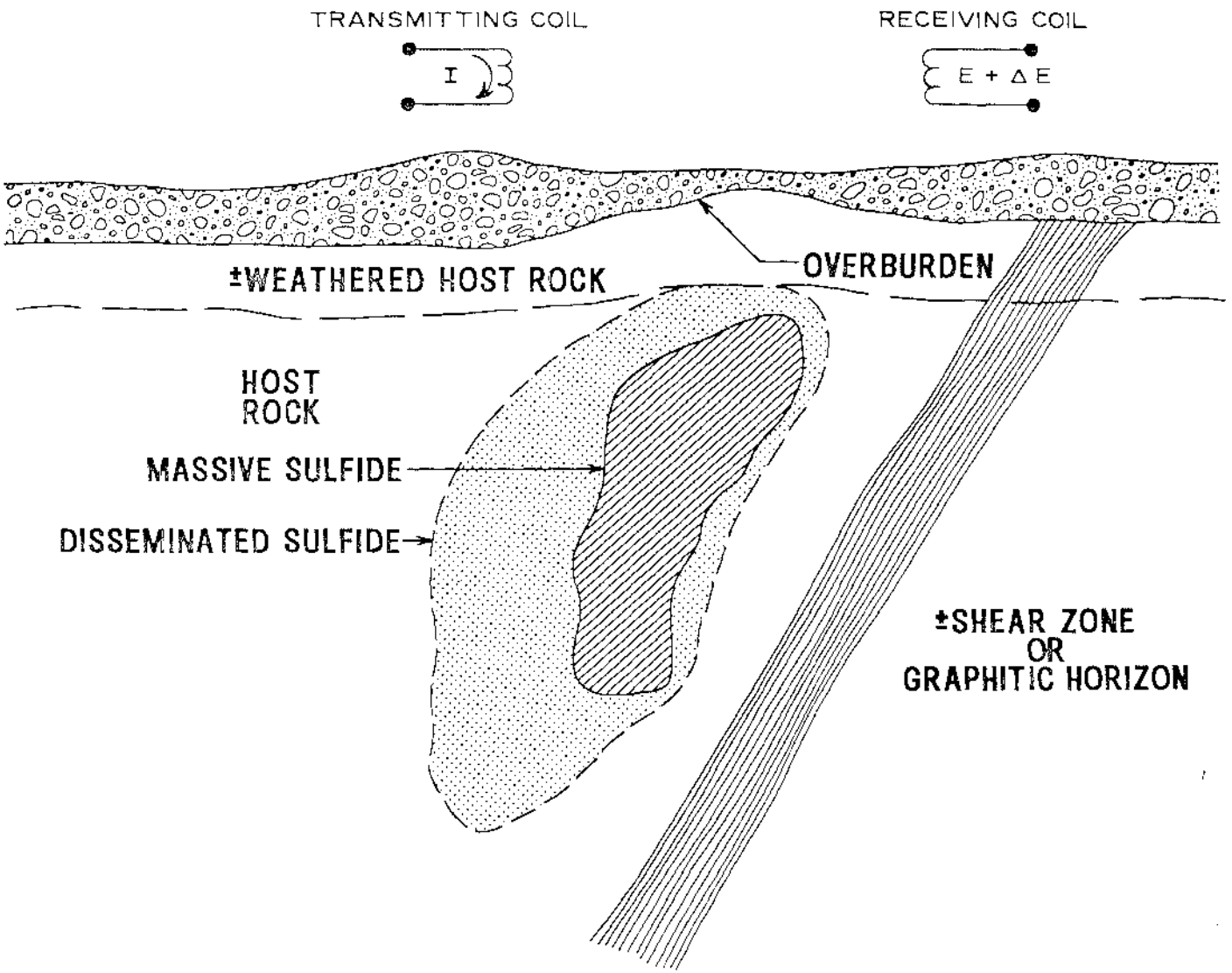

NATURAL MAGNETIC FIELD SPECTRUM

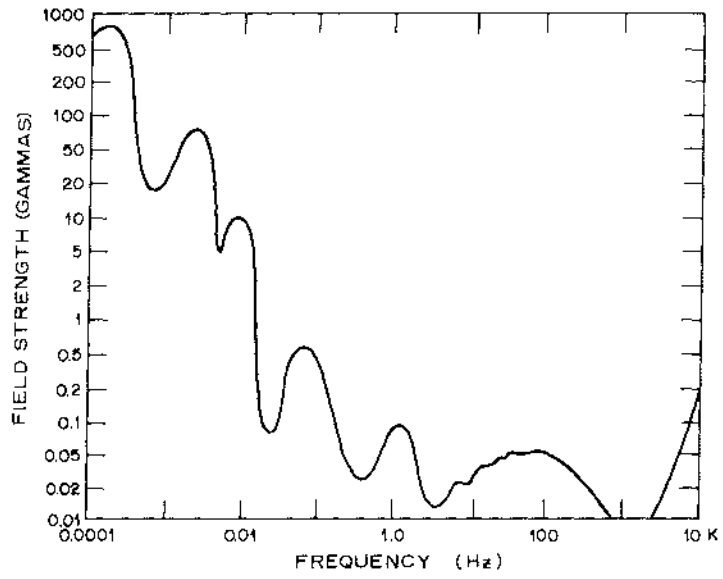

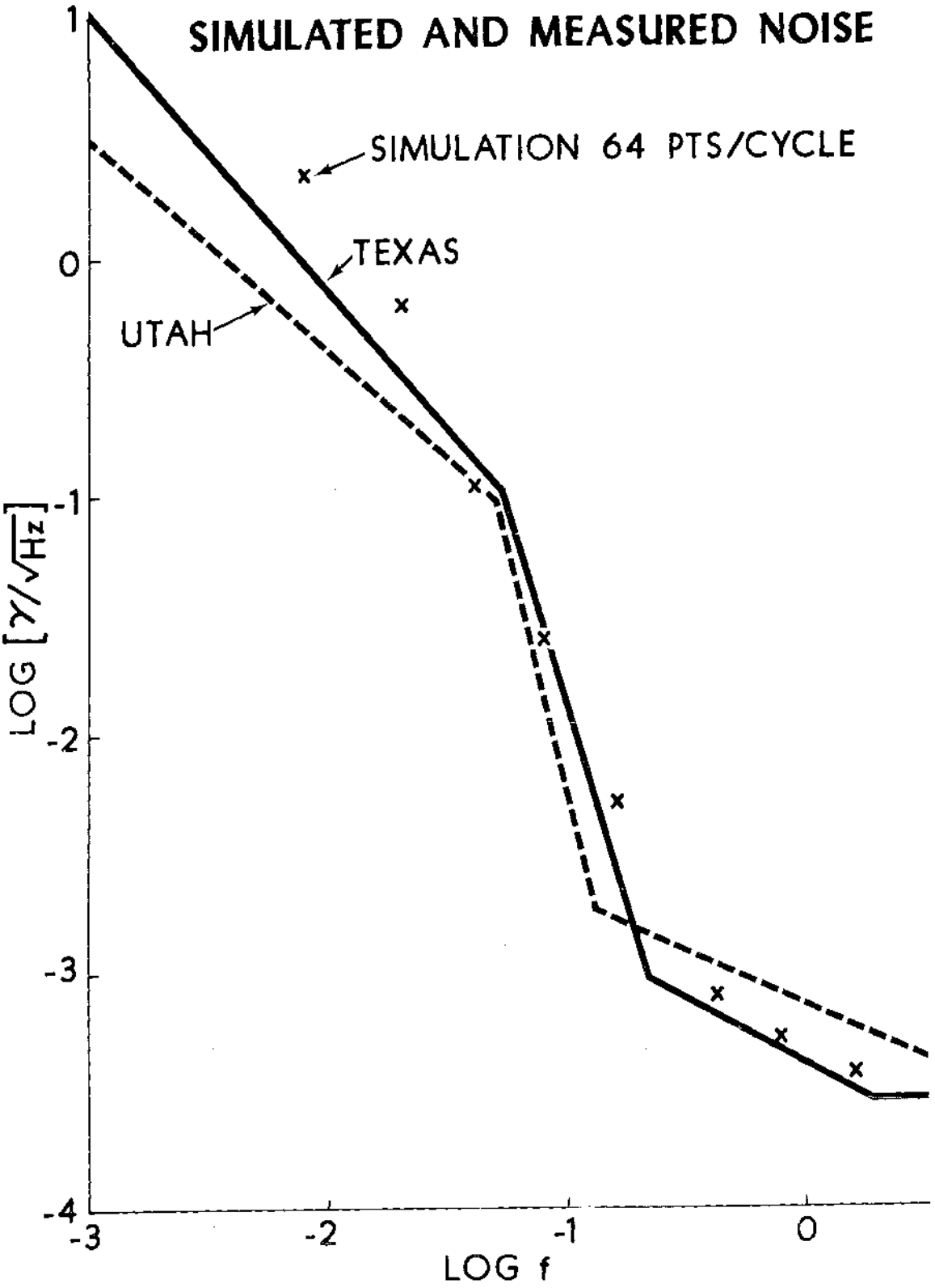
SIMULATED AND MEASURED NOISE
SIMULATION 64 PTS/CYCLE
TEXAS
UTAH
1
0
-1
-2
-3
-4
LOG [γ/√Hz]
-3
-2
-1
0
LOG f

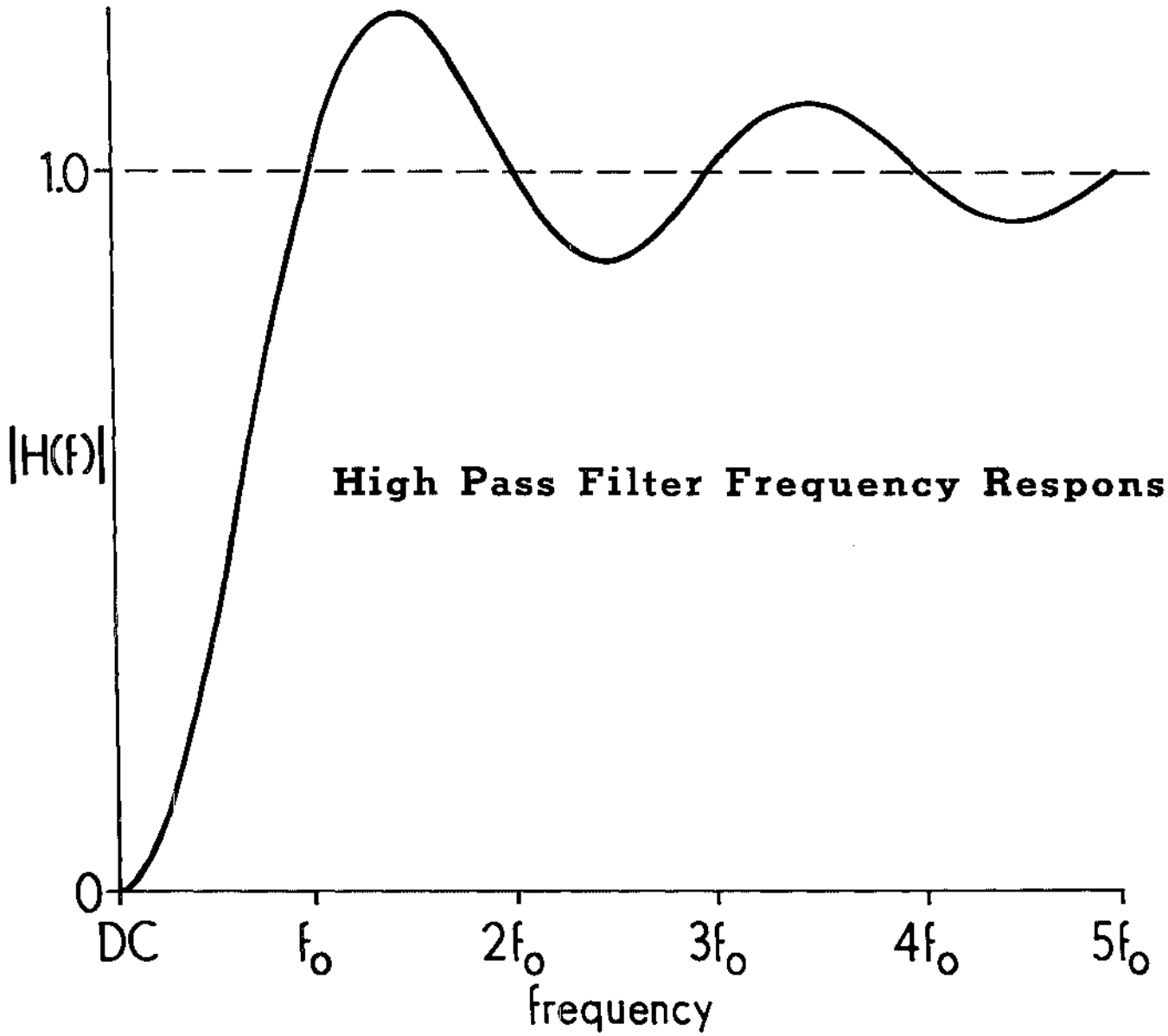

High Pass Filter Frequency Response

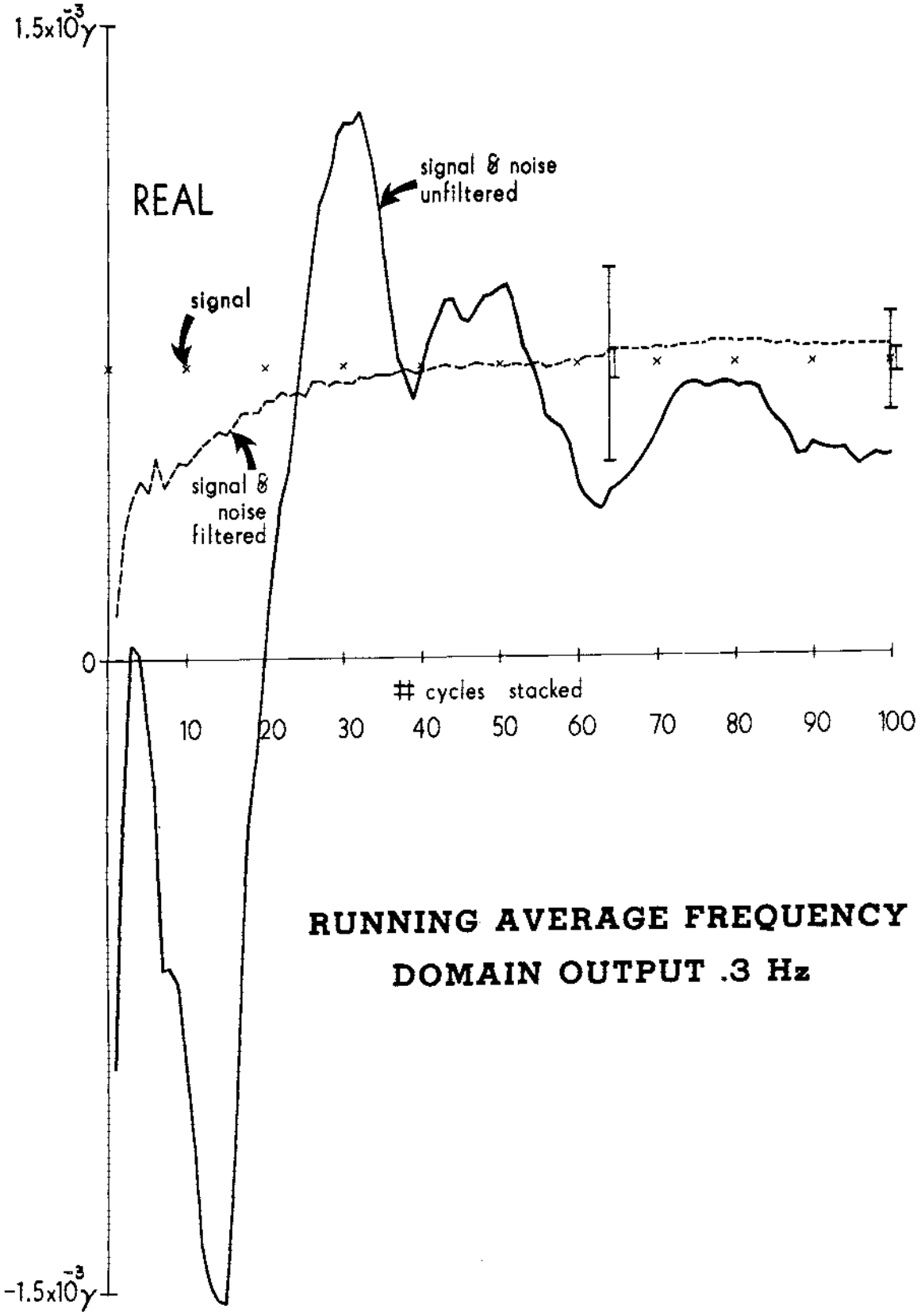

RUNNING AVERAGE FREQUENCY DOMAIN OUTPUT .3 Hz

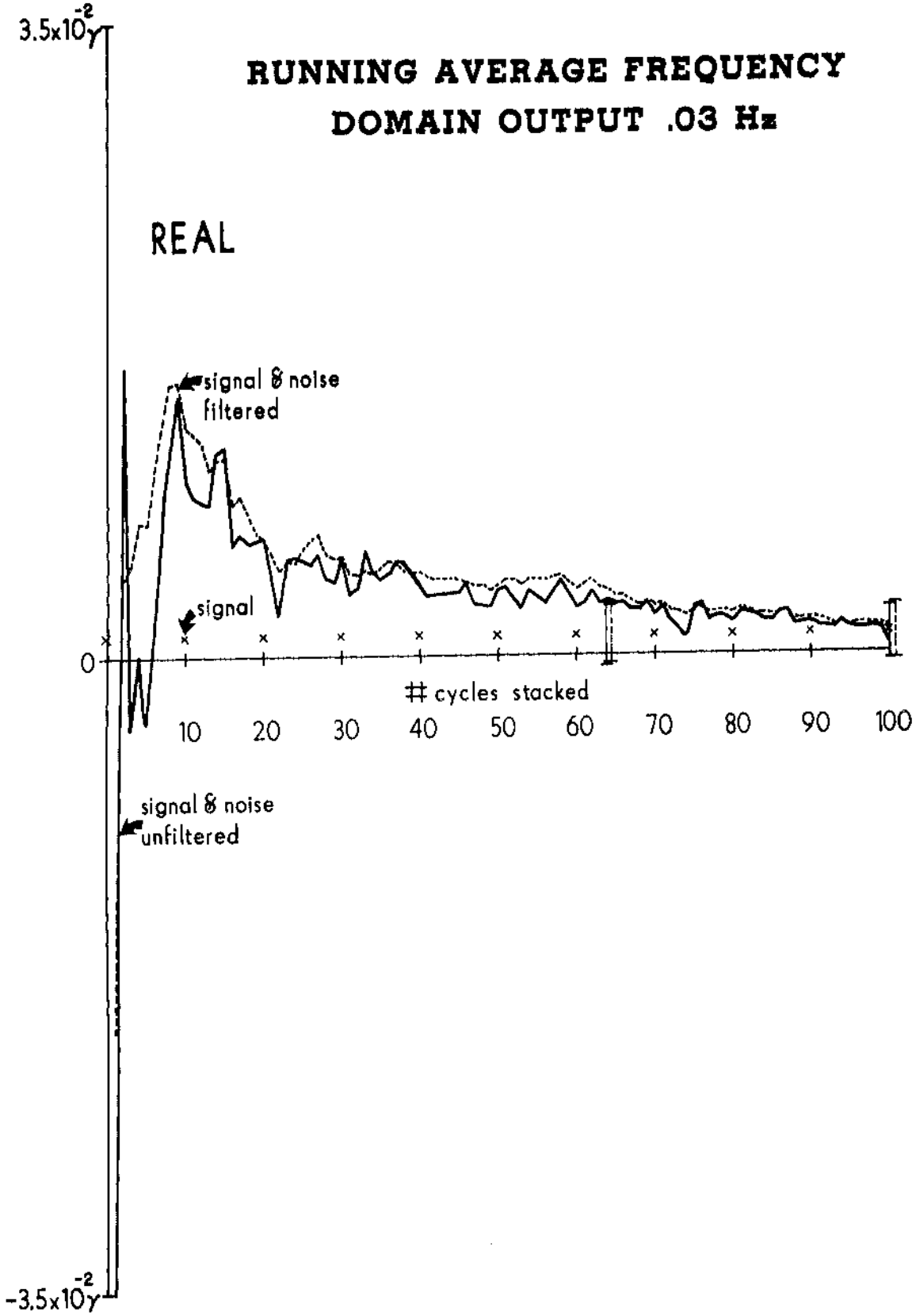
RUNNING AVERAGE FREQUENCY DOMAIN OUTPUT .03 Hz
REAL
3.5x10^-2 γ
-3.5x10^-2 γ
0
signal & noise filtered
signal
signal & noise unfiltered
cycles stacked
10
20
30
40
50
60
70
80
90
100

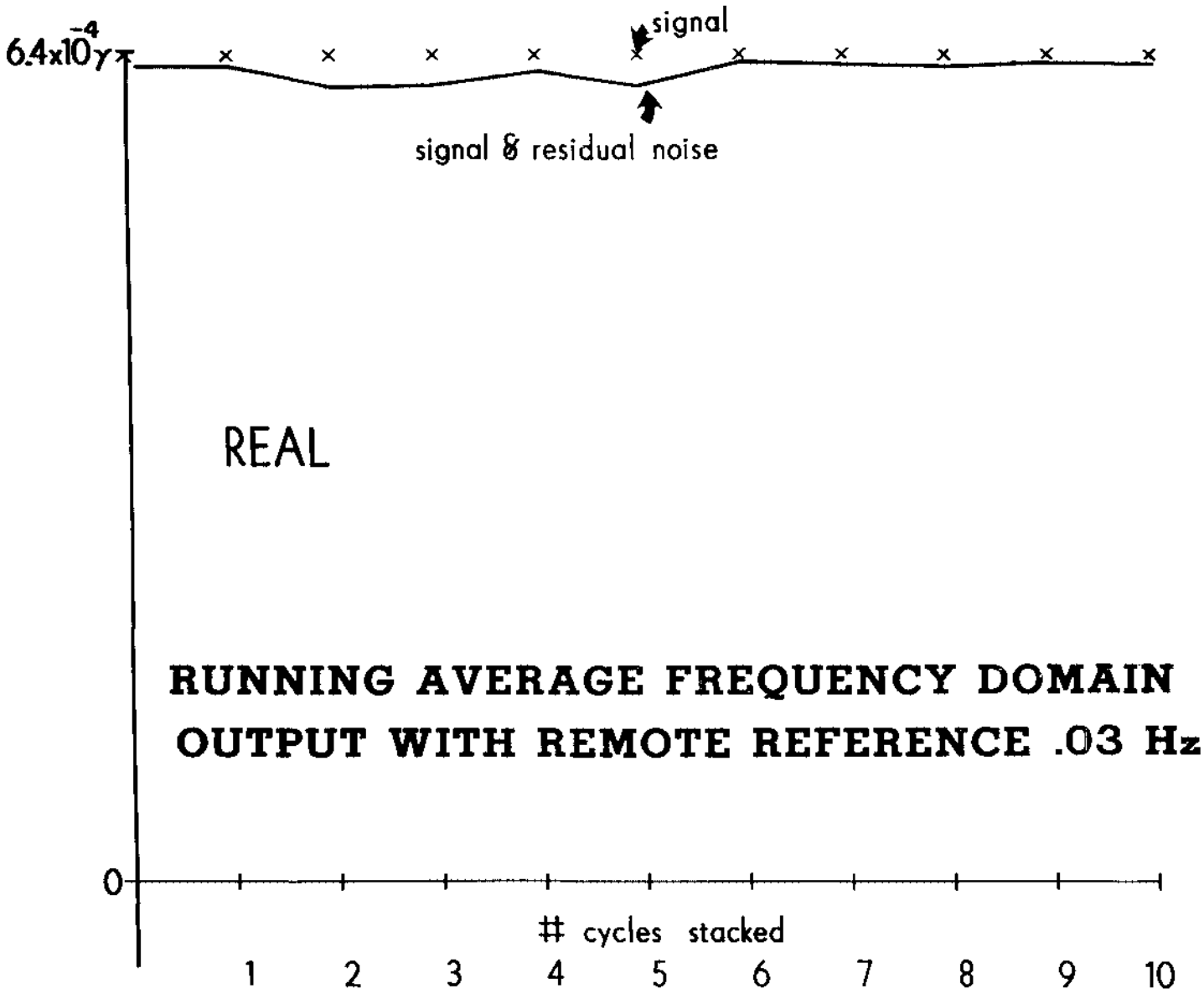
signal
6.4x10⁻⁴γ
signal & residual noise
REAL
RUNNING AVERAGE FREQUENCY DOMAIN
OUTPUT WITH REMOTE REFERENCE .03 Hz
0
cycles stacked
1
2
3
4
5
6
7
8
9
10

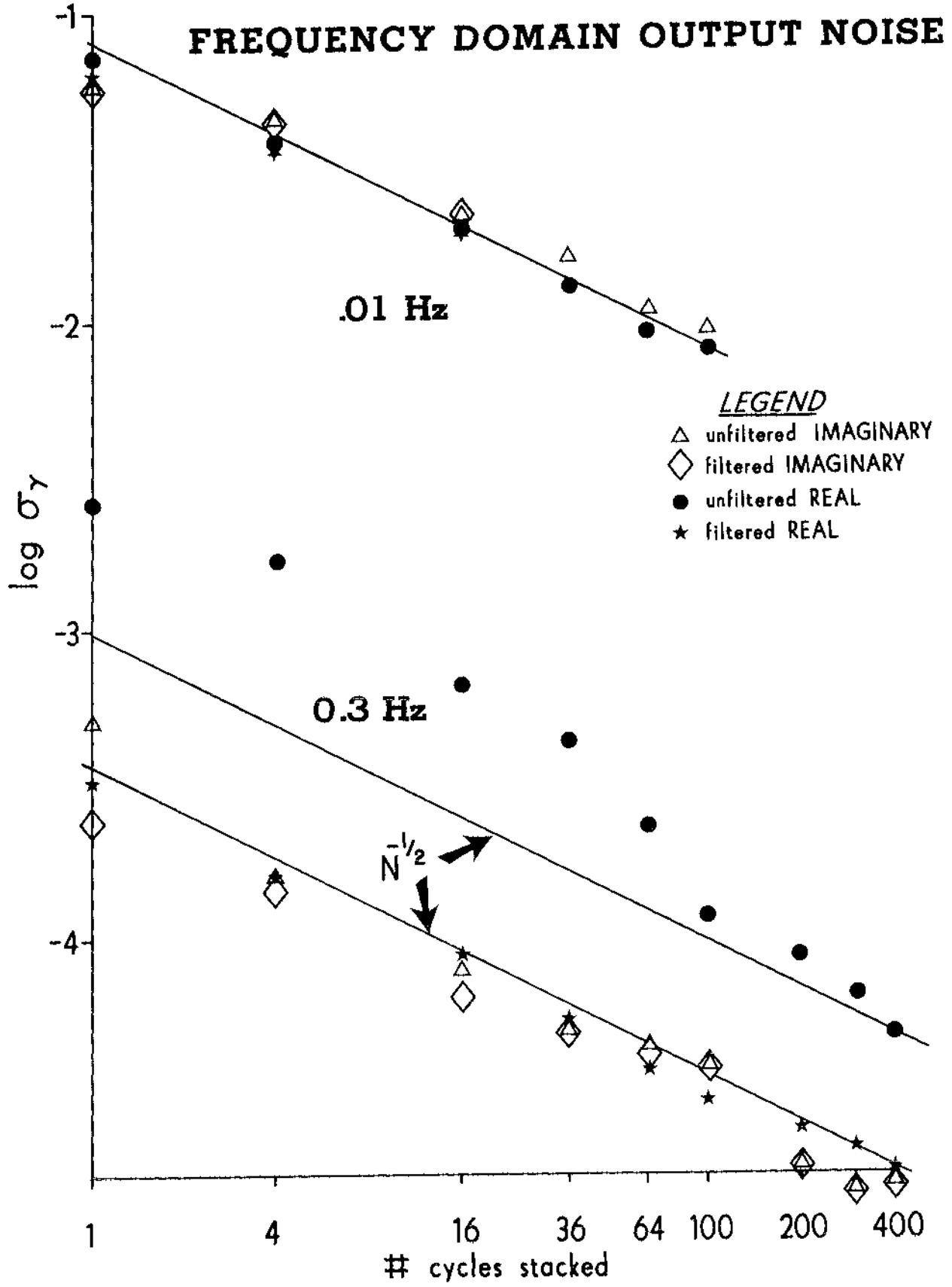
FREQUENCY DOMAIN OUTPUT NOISE
-1
-2
-3
-4
log σ_Y
.01 Hz
0.3 Hz
N^-1/2
LEGEND
unfiltered IMAGINARY
filtered IMAGINARY
unfiltered REAL
filtered REAL
1
4
16
36
64
100
200
400
cycles stacked

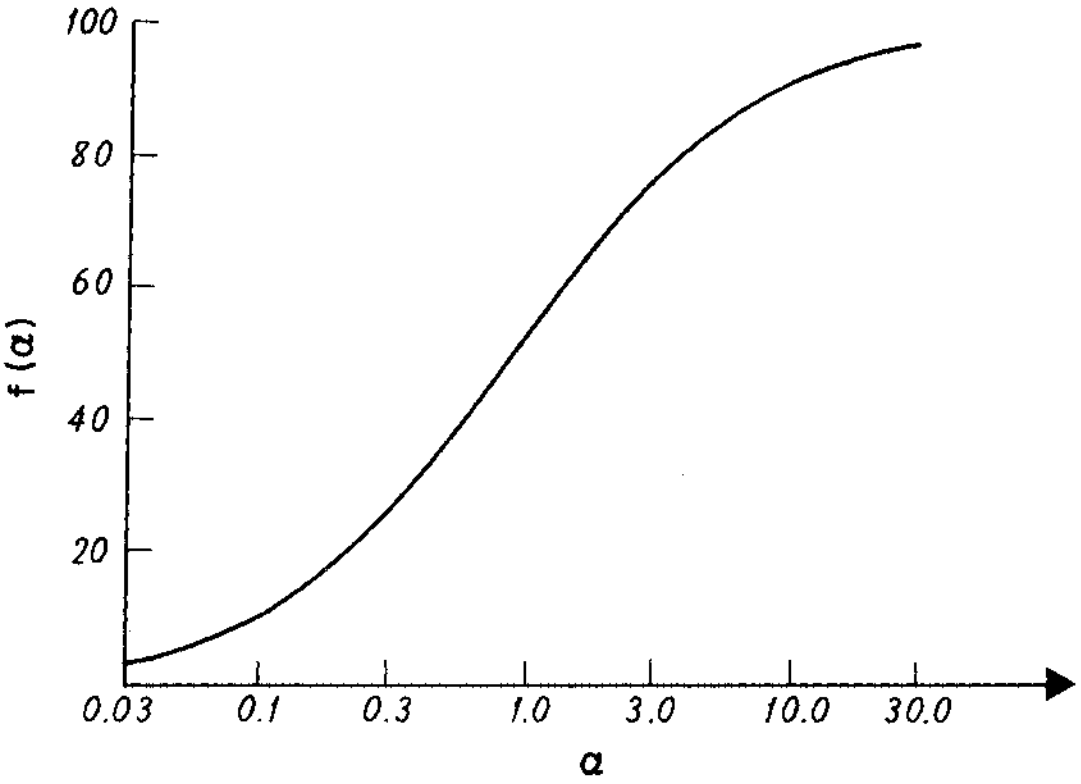
100
80
60
40
20
f(α)
0.03
0.1
0.3
1.0
3.0
10.0
30.0
α

TRANSMITTED AND RECEIVED WAVEFORMS

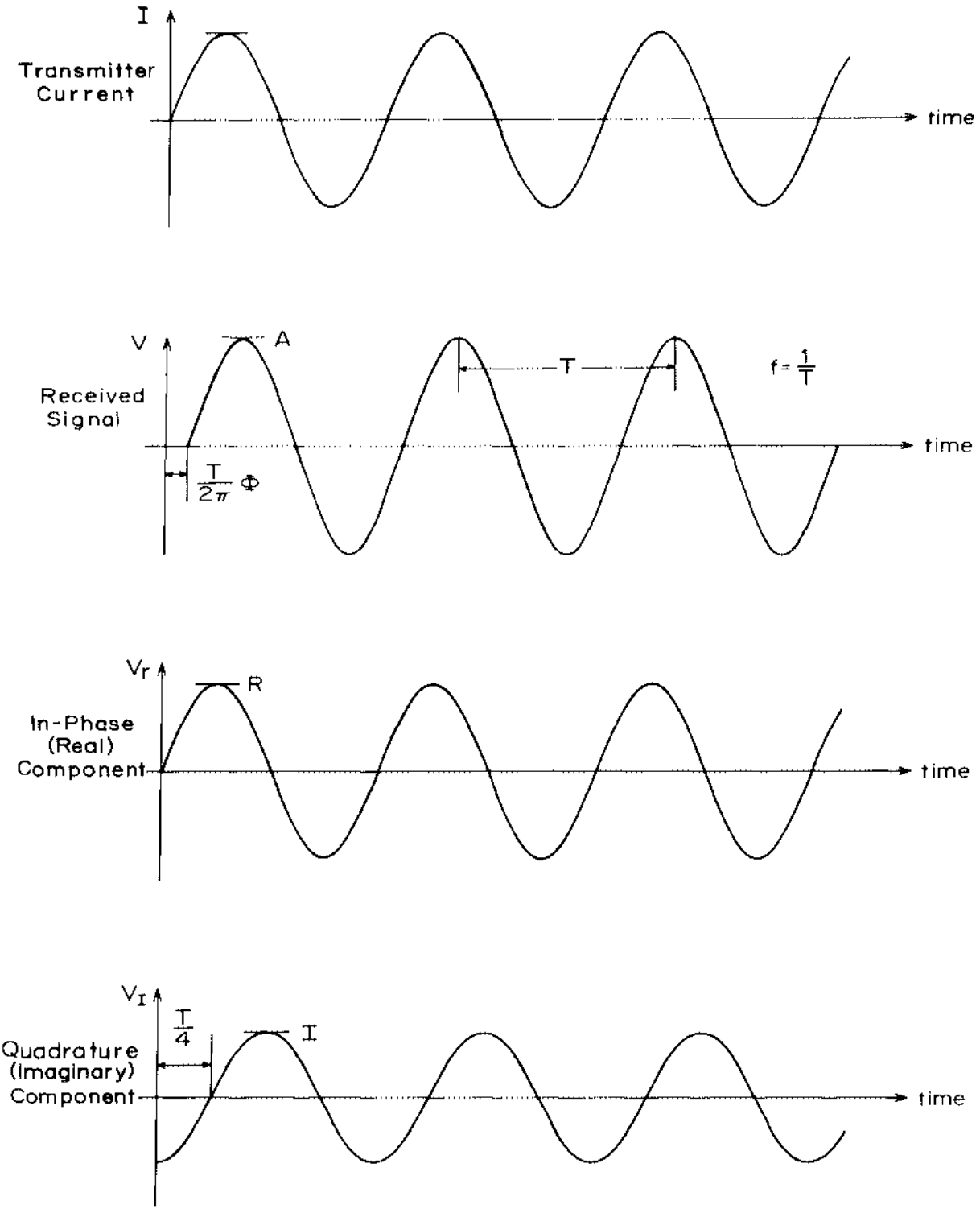

TRANSMITTED AND RECEIVED WAVEFORMS

TRANSMITTER CURRENT

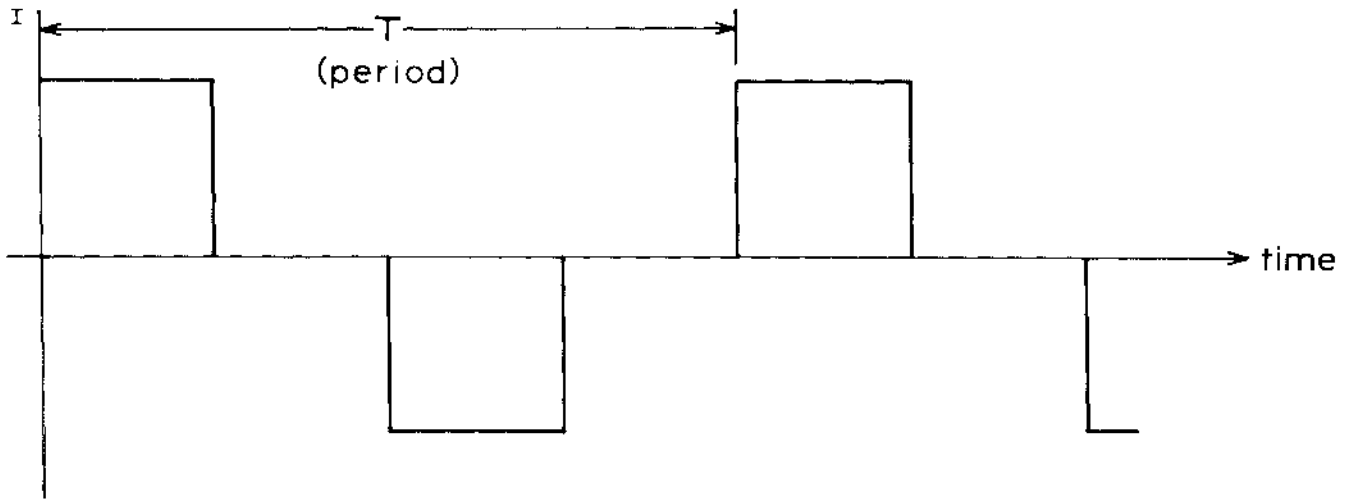

RECEIVED SIGNAL

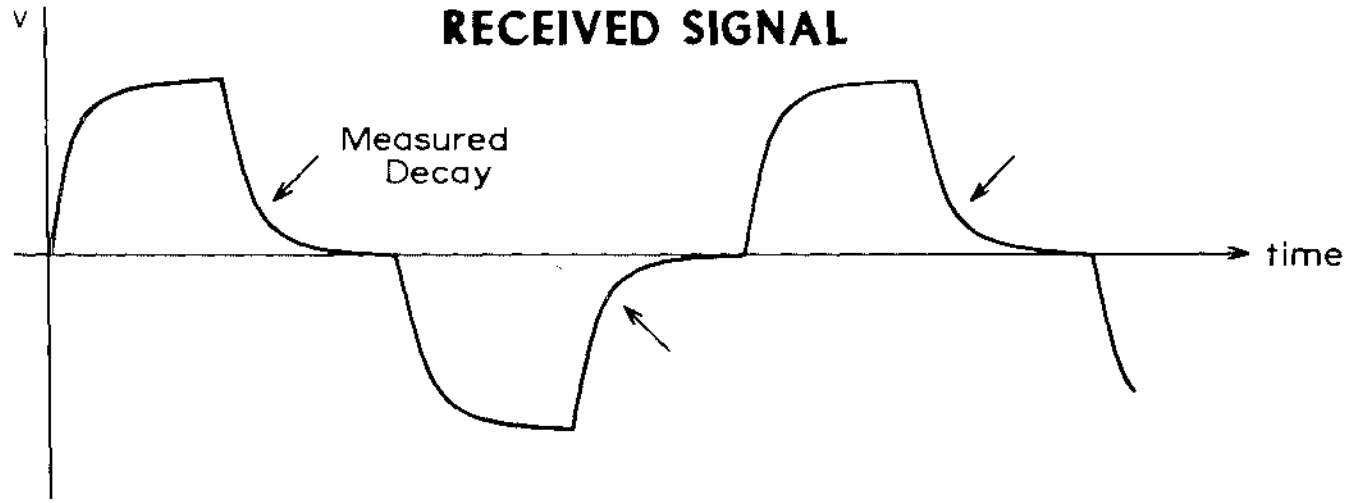

BASIC GROUND EM METHODS

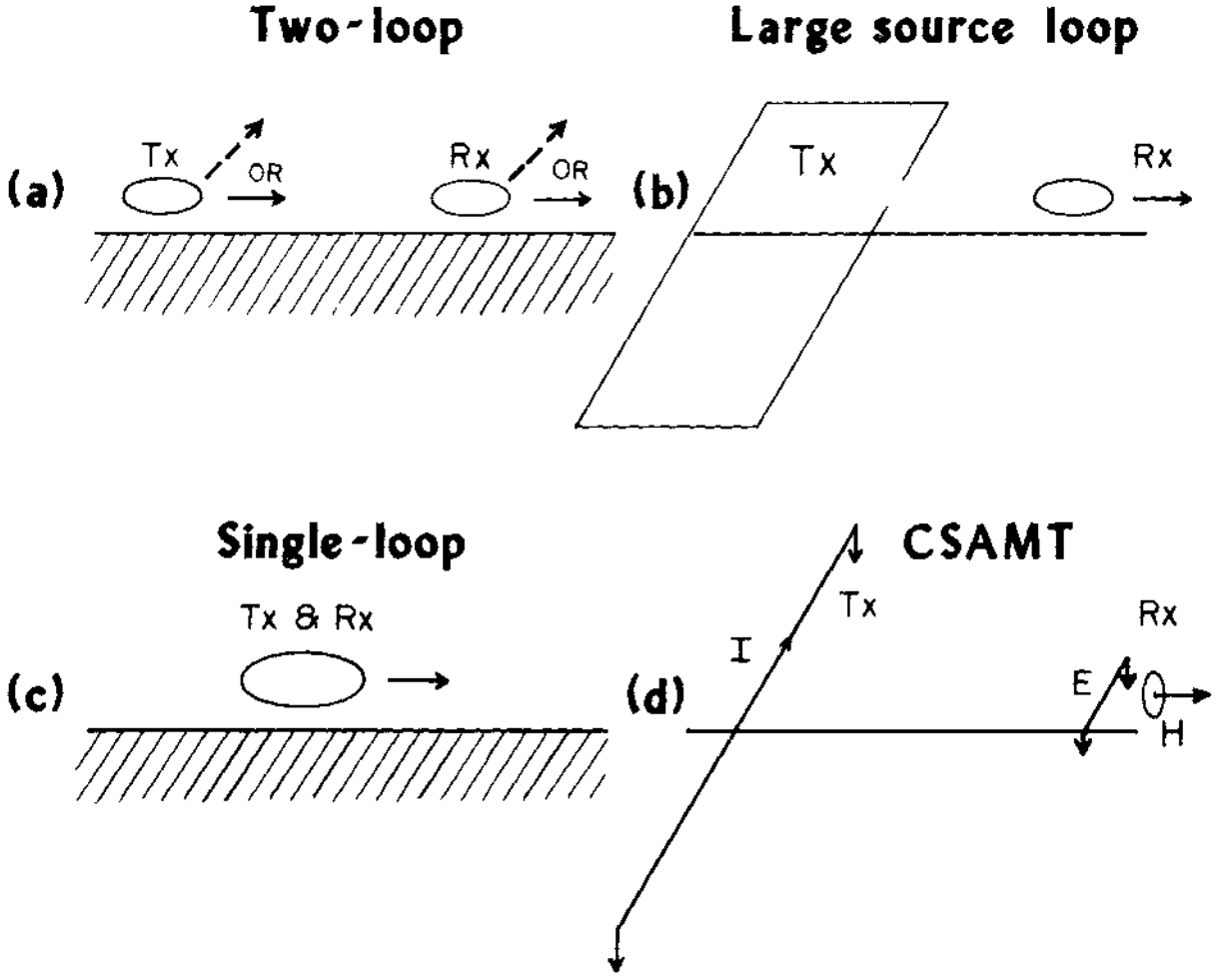

PROFILE I (4000 N)
FIELD DATA

APPARENT RESISTIVITY
TM mode (E-W electric field)

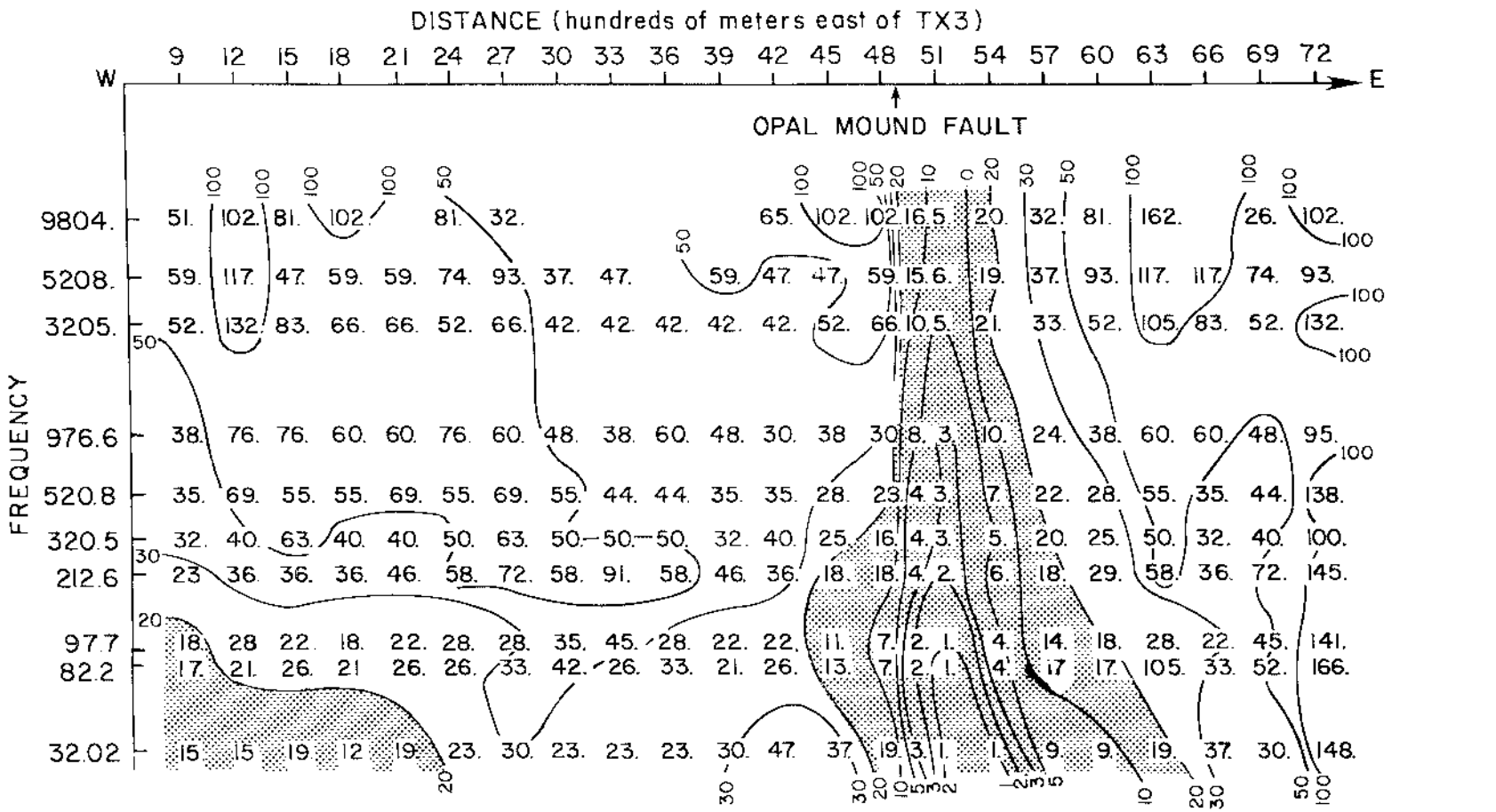

PROFILE 1 (4000 N)
RESPONSE TO CSAMT MODEL

TM mode (E-W electric field)

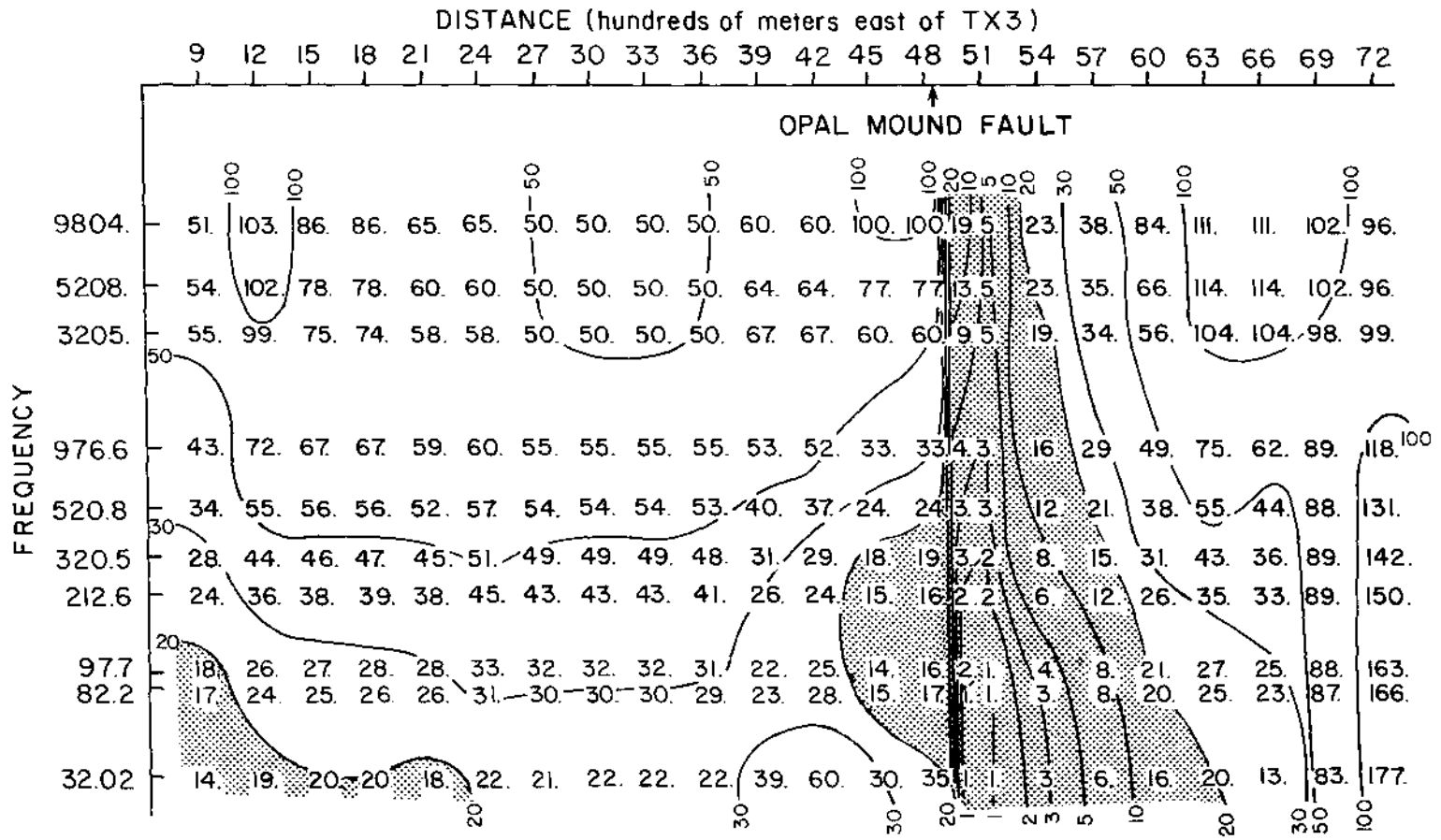

CSAMT 2D MODEL (4000N)

VERTICAL EXAGGERATION IS 2:1

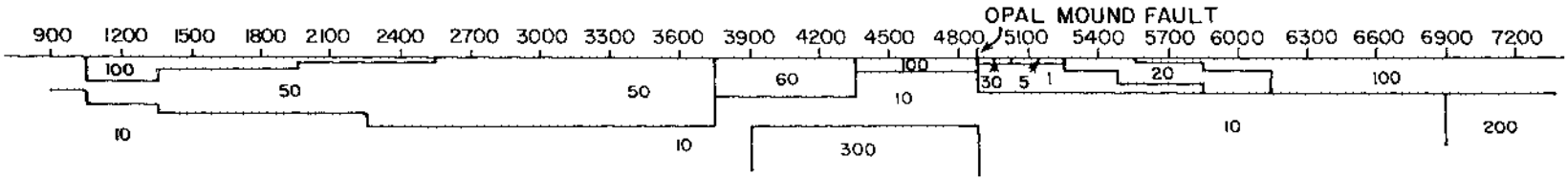

DIPOLE-DIPOLE RESISTIVITY MODEL (4000 N)

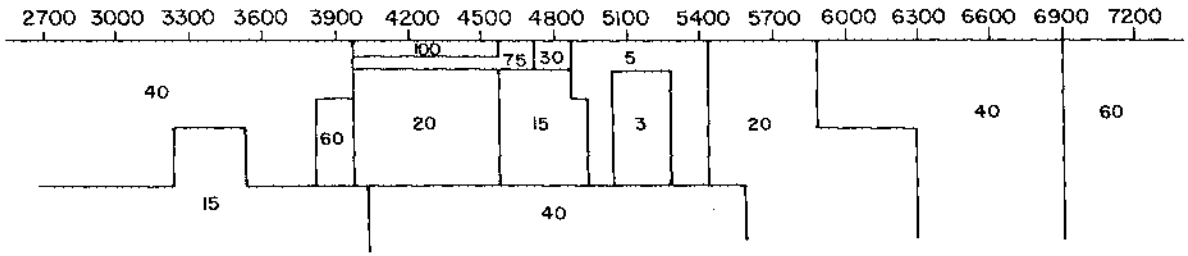

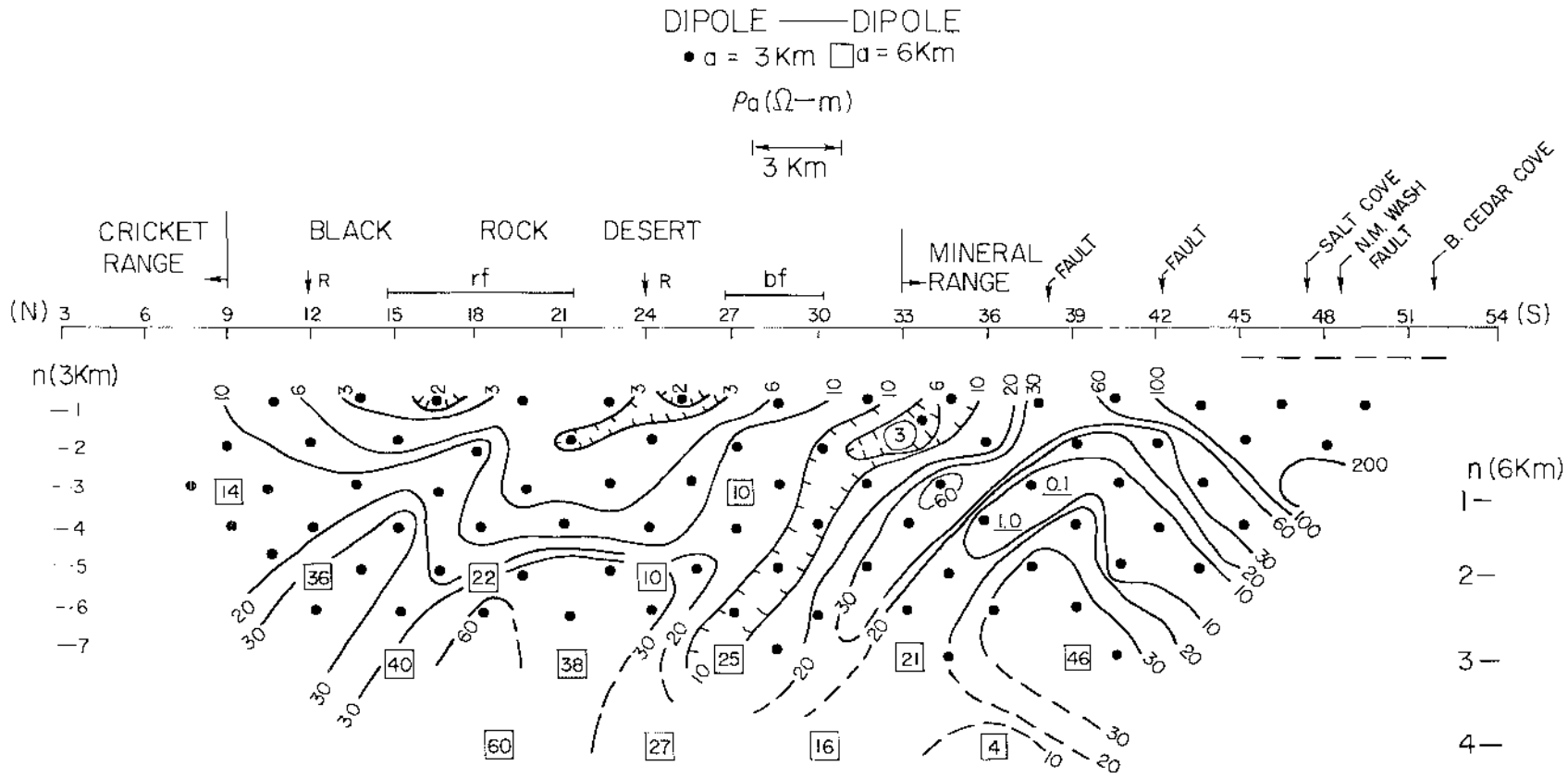
DIPOLE ——DIPOLE
• a = 3Km □a = 6Km
ρa (Ω—m)
3 Km
CRICKET RANGE
BLACK
ROCK
DESERT
MINERAL RANGE
FAULT
FAULT
SALT COVE
N.M. WASH FAULT
B. CEDAR COVE
R
rf
R
bf
(N) 3 6 9 12 15 18 21 24 27 30 33 36 39 42 45 48 51 54 (S)
n(3Km)
1
2
3
4
5
6
7
n(6Km)
1
2
3
4

Field data-North end Roosevelt
3km dipole-dipole profile

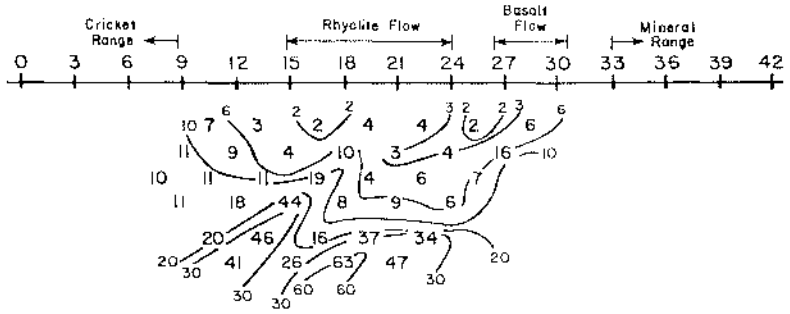

Alpha media resistivity distribution — 3 α centers

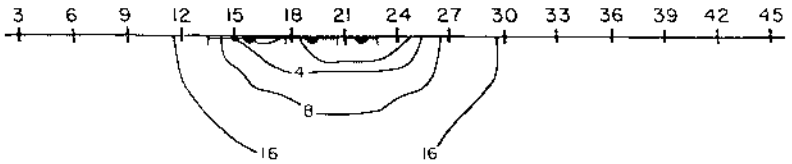

Alpha media resistivity distribution — 5 α centers

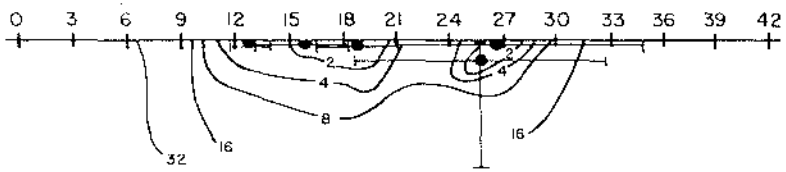

Best fit alpha center pseudosection — 3 α centers

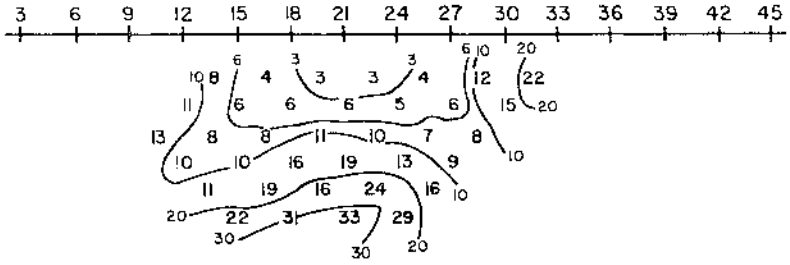

Best fit alpha center pseudosection — 5 α centers

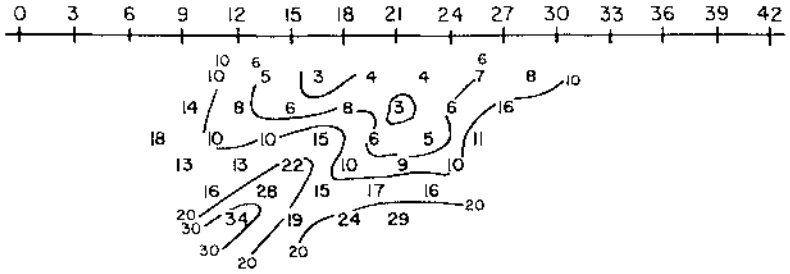

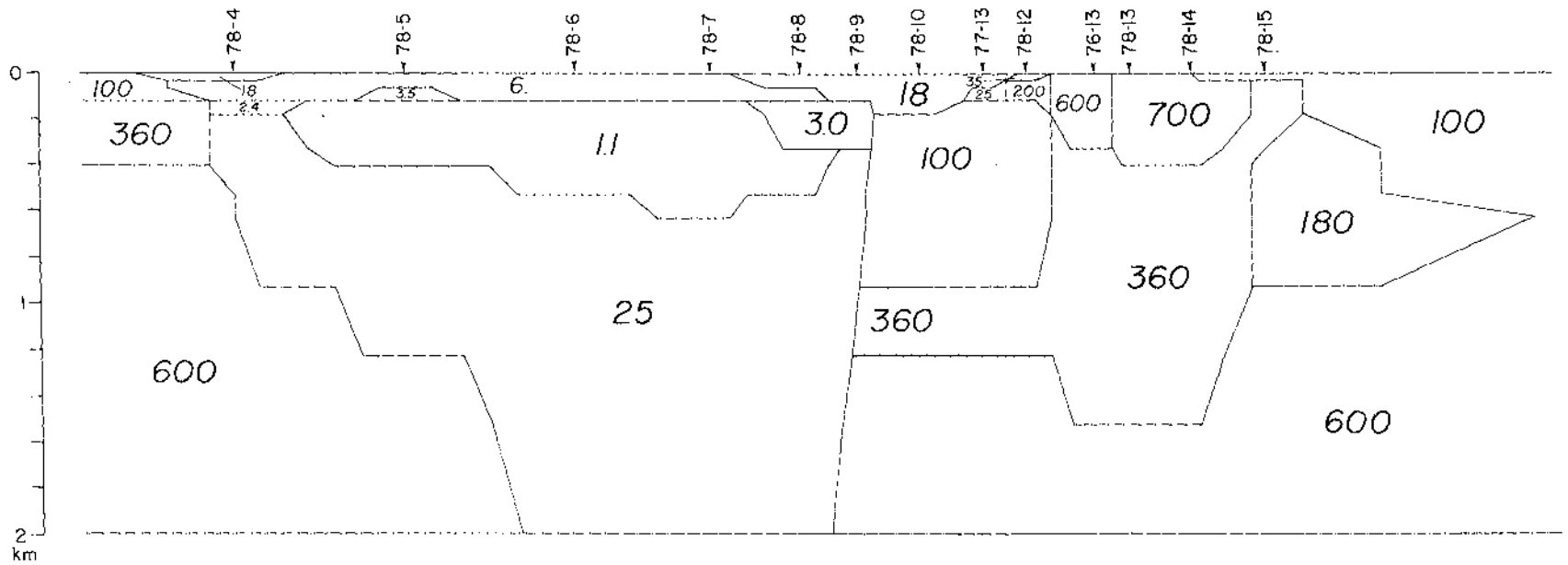

2-D TM BEST FIT
FINITE ELEMENT
CROSS-SECTION
LINE B-B'

VERT. EXAG.
6:1

0 5km

1400

3000

OBSERVED APPARENT RESISTIVITY B-B'

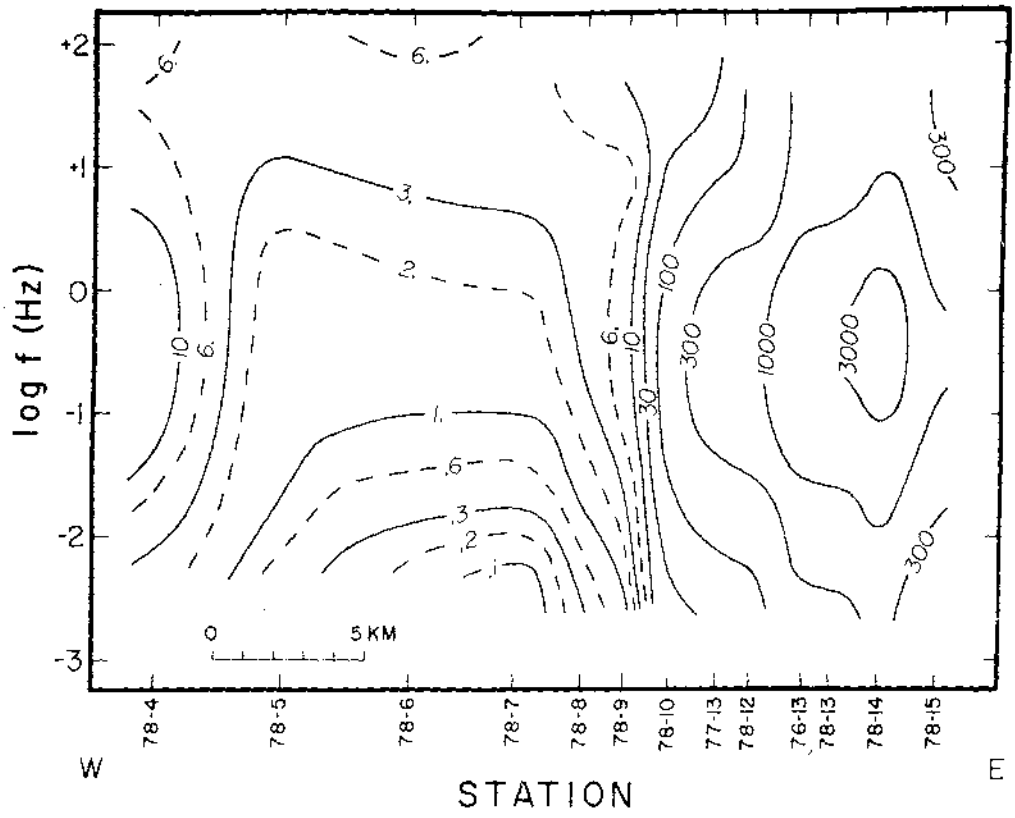

OBSERVED IMPEDANCE PHASE B-B'

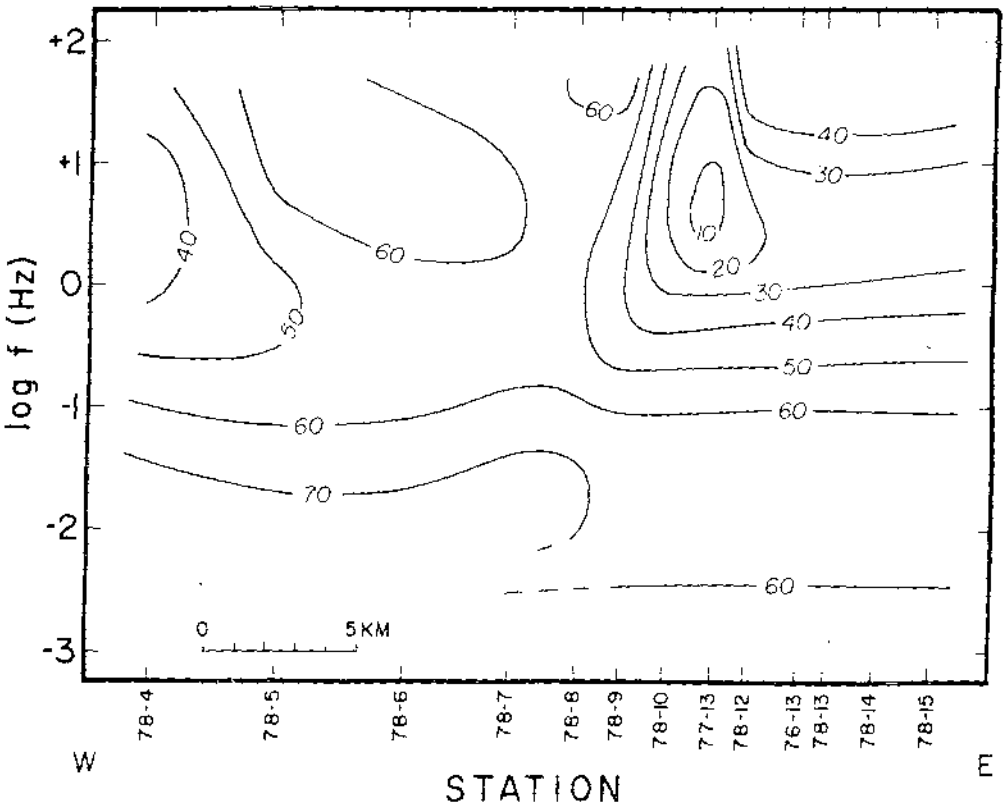

MODELED APPARENT RESISTIVITY B-B'

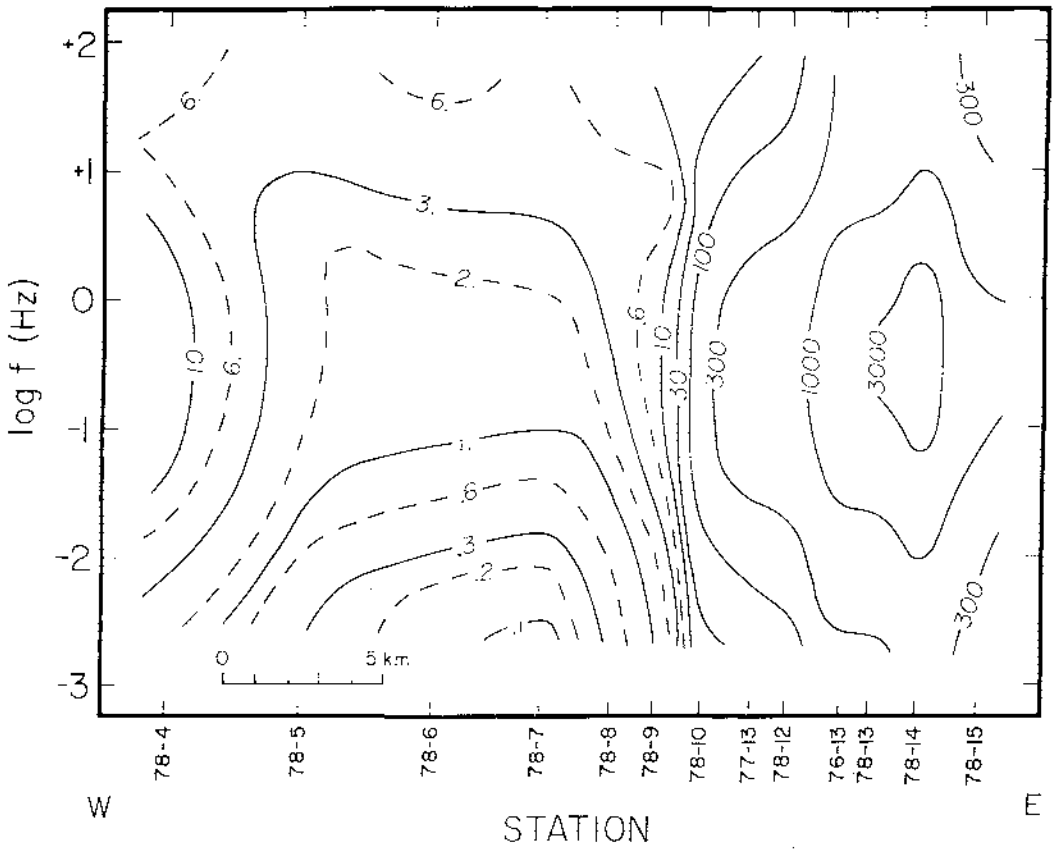

MODELED IMPEDANCE PHASE B-B'

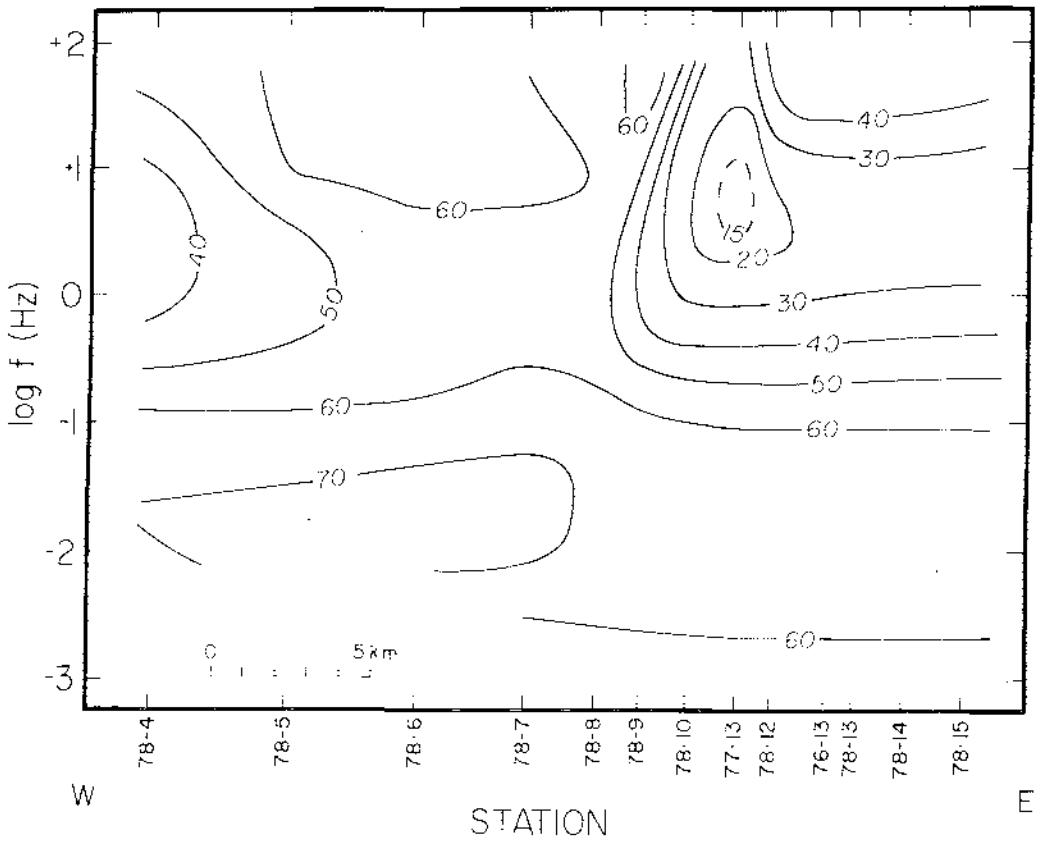

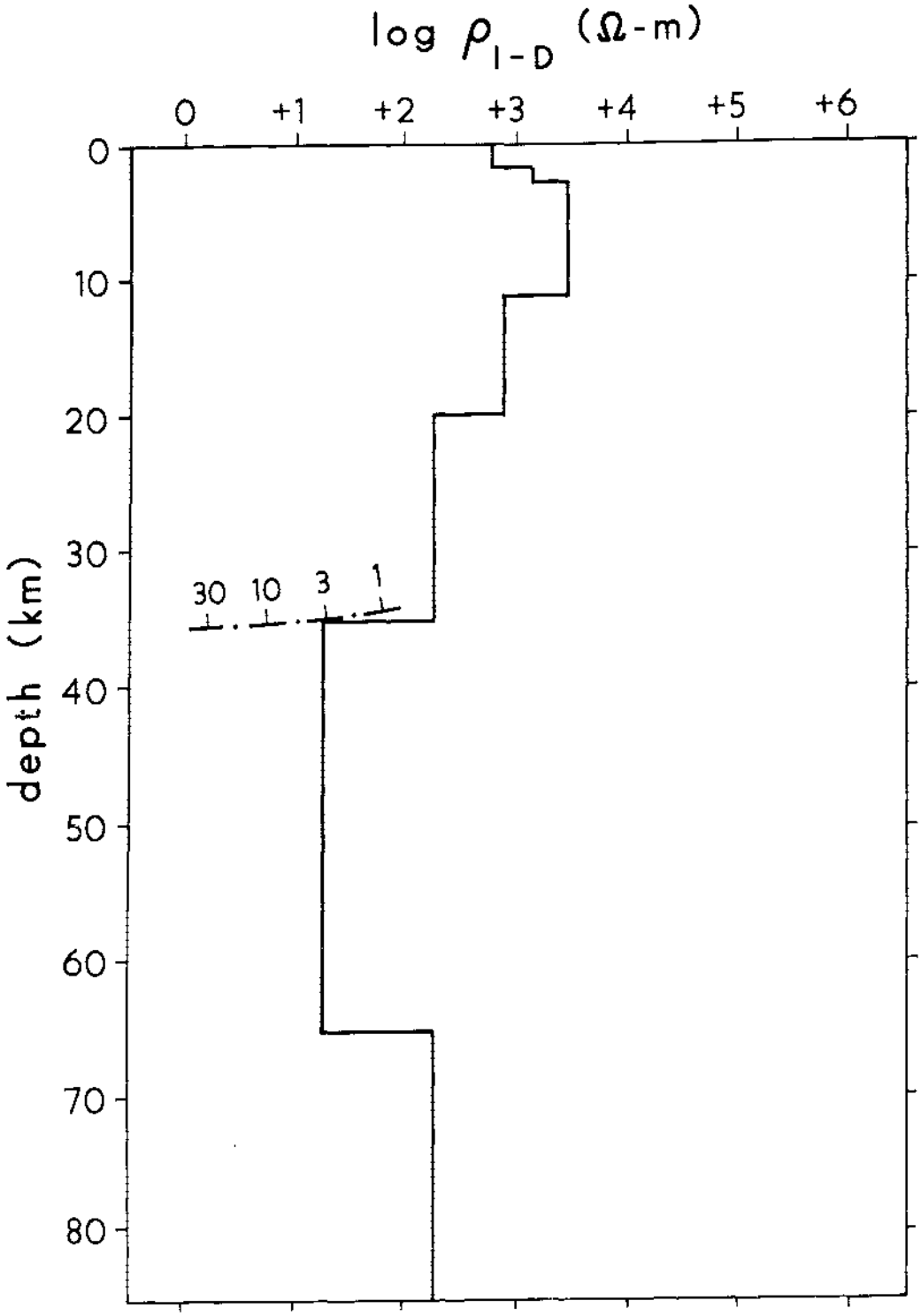
log ρ_{1-D} (Ω-m)
0
+1
+2
+3
+4
+5
+6
0
10
20
30
40
50
60
70
80
depth (km)
30
10
3
1

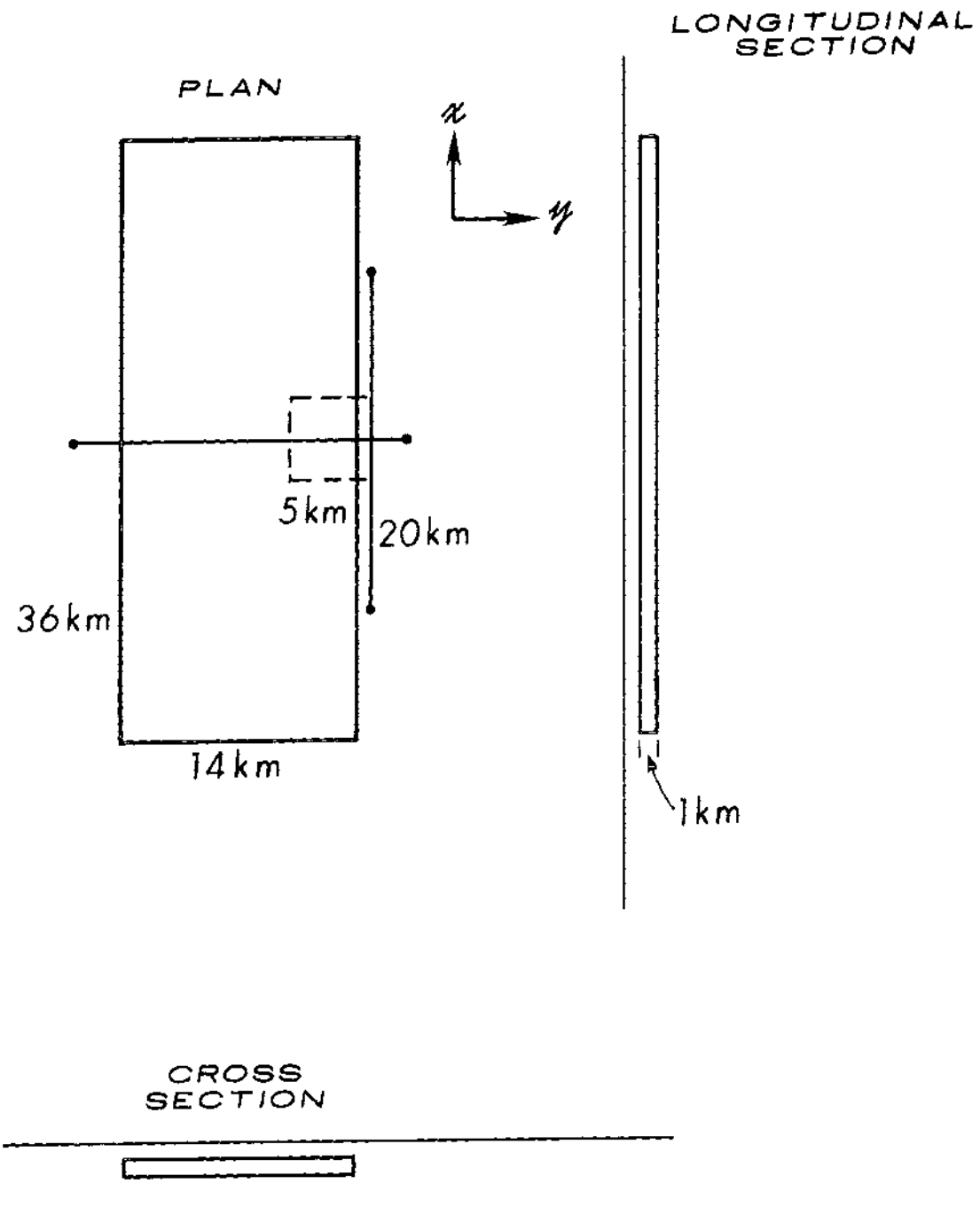

VALLEY FILL MODEL

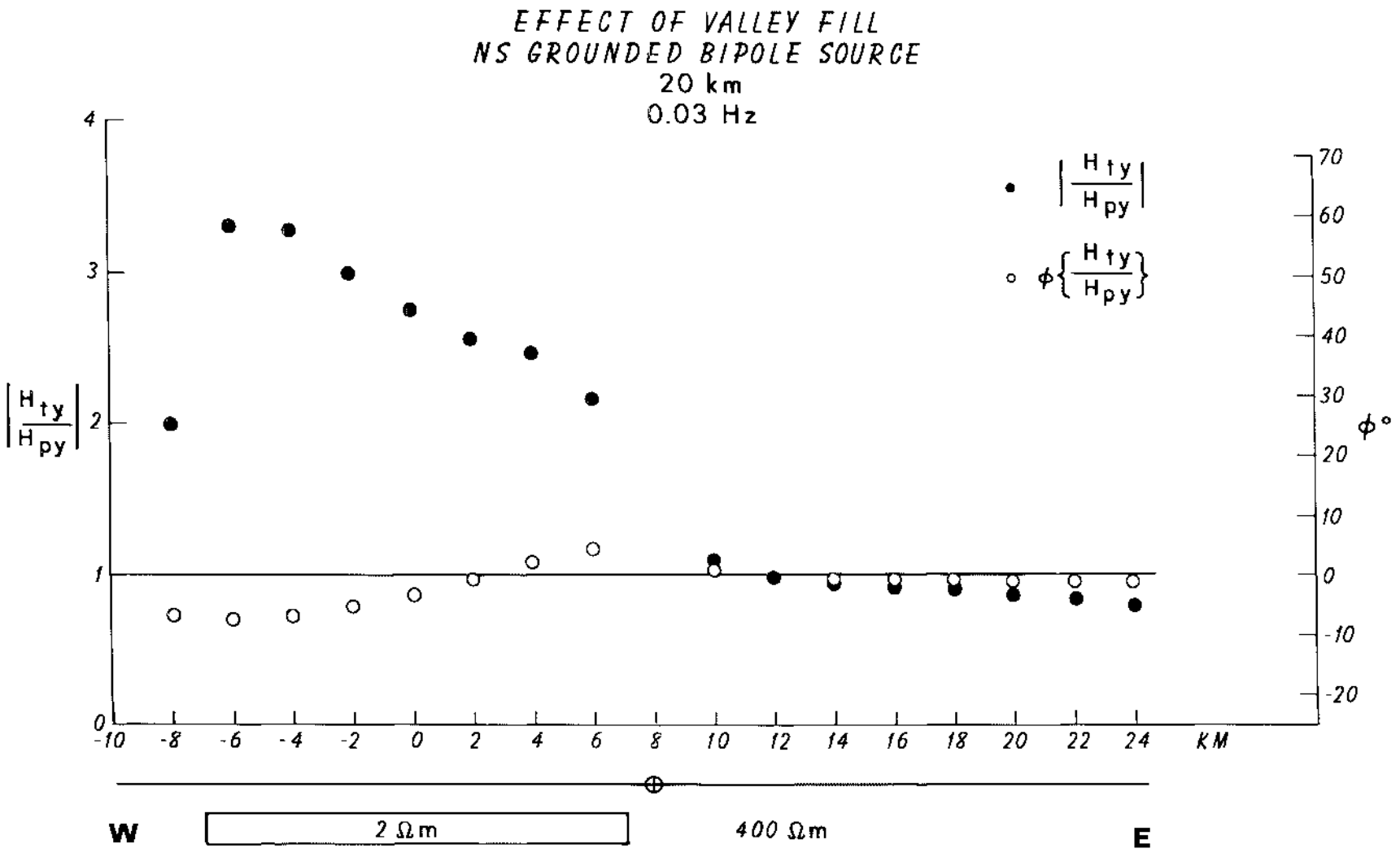
EFFECT OF VALLEY FILL
NS GROUNDED BIPOLE SOURCE
20 km
0.03 Hz
$\left|\frac{H_{ty}}{H_{py}}\right|$
$\phi\left\{\frac{H_{ty}}{H_{py}}\right\}$
$\phi°$
KM
W
2 Ωm
400 Ωm
E

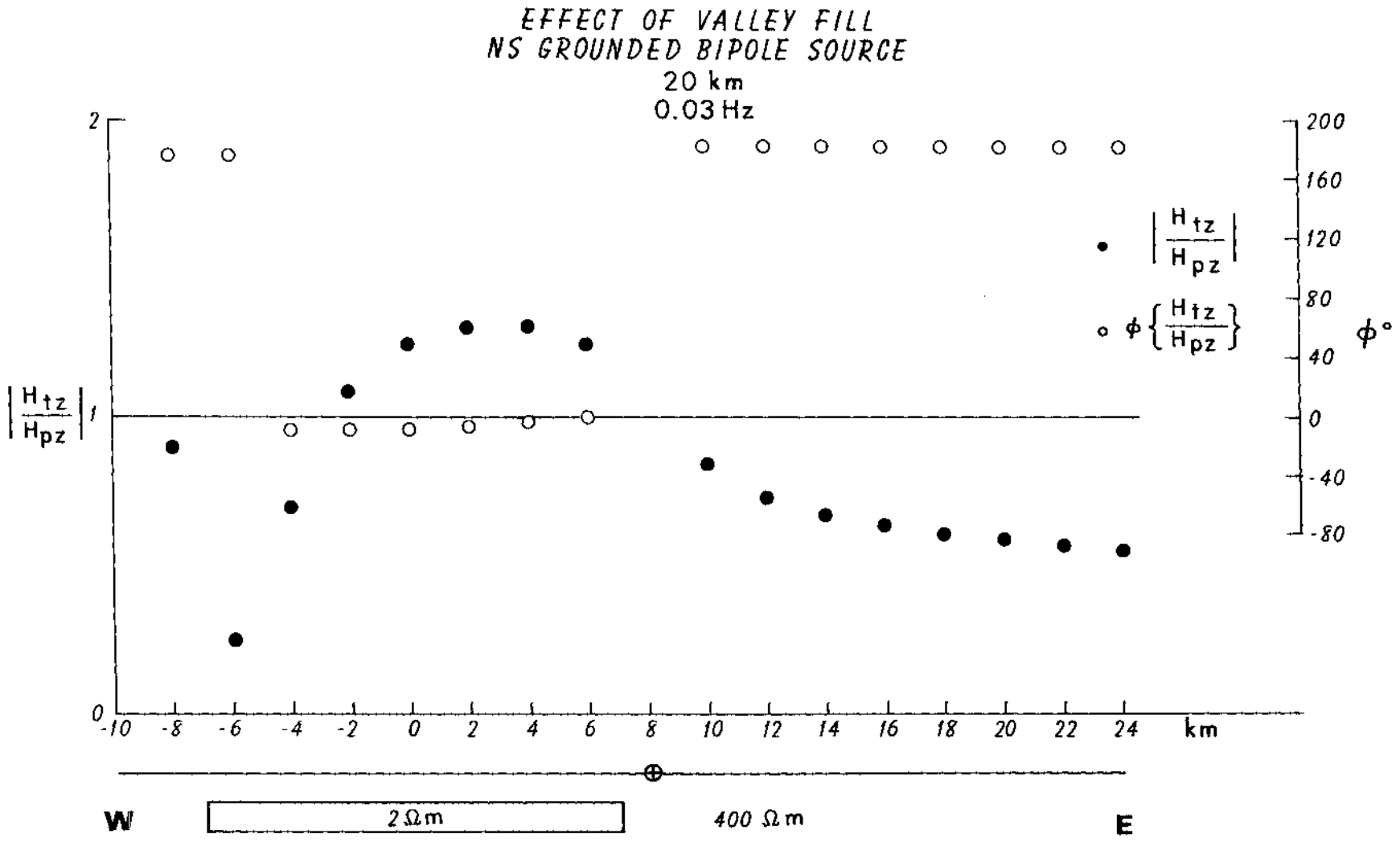
EFFECT OF VALLEY FILL
NS GROUNDED BIPOLE SOURCE
20 km
0.03 Hz
2
1
0
|Htz/Hpz|
200
160
120
80
40
0
-40
-80
φ°
|Htz/Hpz|
φ{Htz/Hpz}
-10 -8 -6 -4 -2 0 2 4 6 8 10 12 14 16 18 20 22 24
km
W
2 Ω m
400 Ω m
E

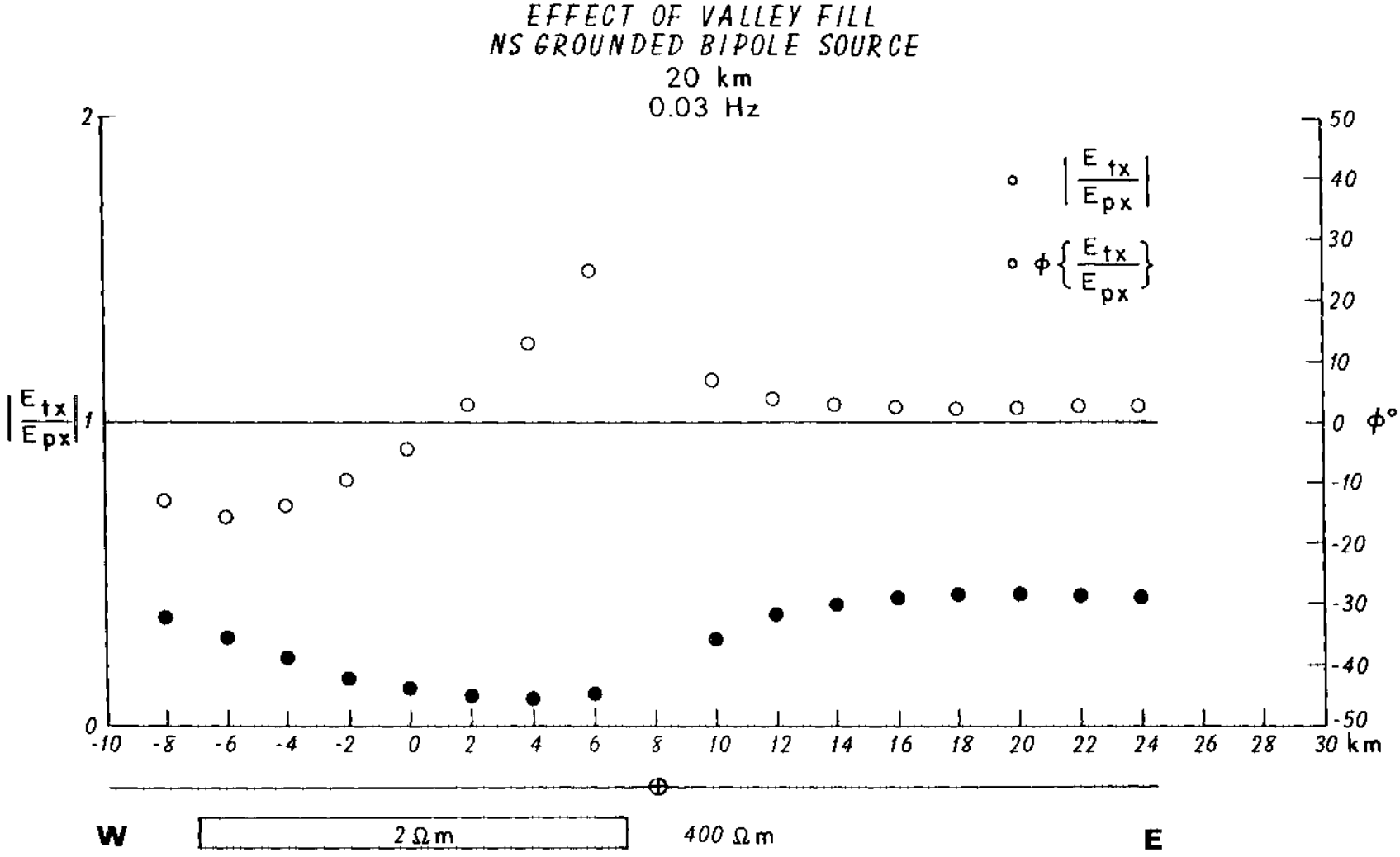
EFFECT OF VALLEY FILL
NS GROUNDED BIPOLE SOURCE
20 km
0.03 Hz
$\left|\frac{E_{tx}}{E_{px}}\right|$
$\phi\left\{\frac{E_{tx}}{E_{px}}\right\}$
$\left|\frac{E_{tx}}{E_{px}}\right|$
$\phi°$
2
1
0
50
40
30
20
10
0
-10
-20
-30
-40
-50
-10 -8 -6 -4 -2 0 2 4 6 8 10 12 14 16 18 20 22 24 26 28 30 km
W
2 Ω m
400 Ω m
E

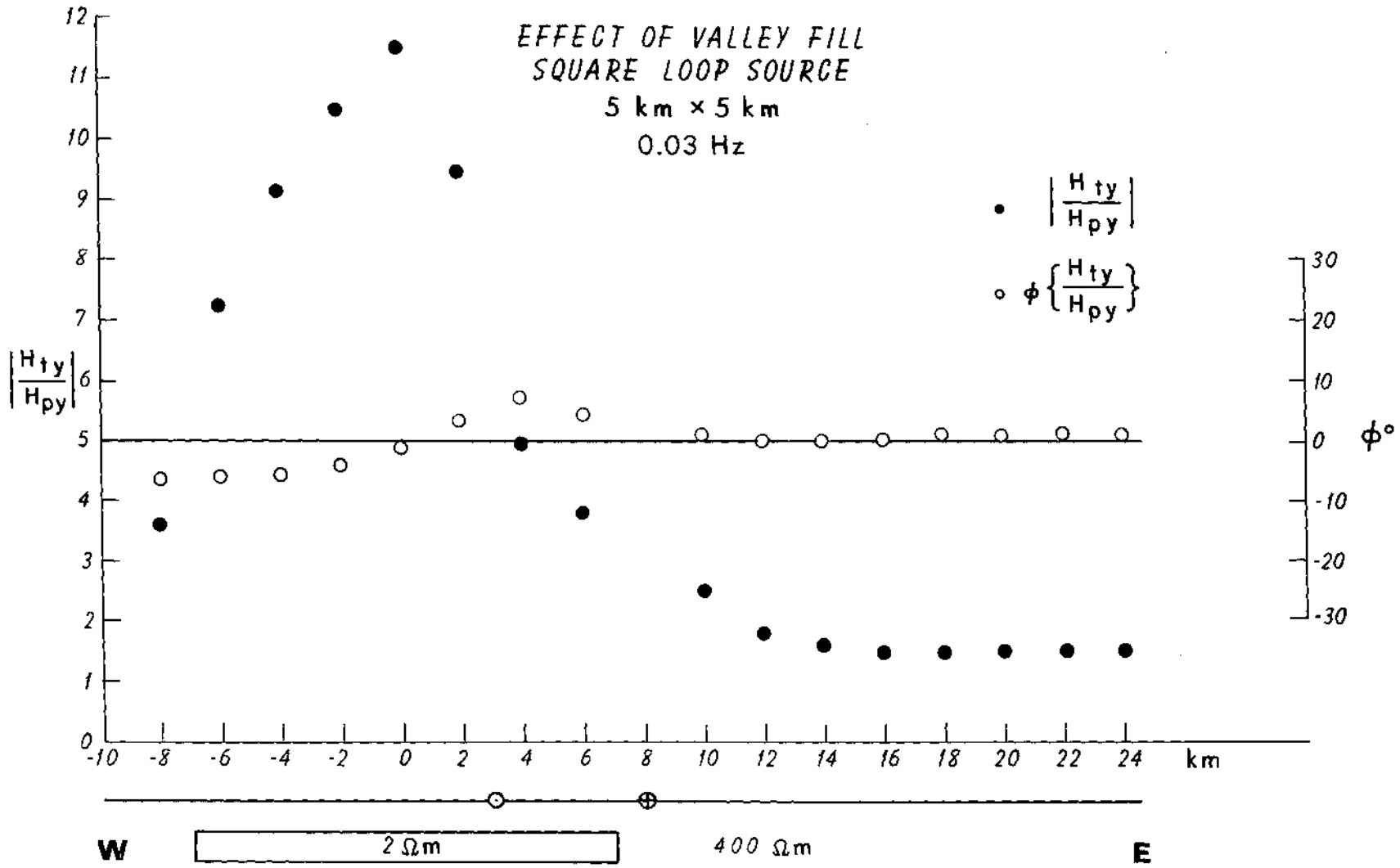
EFFECT OF VALLEY FILL
SQUARE LOOP SOURCE
5 km × 5 km
0.03 Hz
$\left|\frac{H_{ty}}{H_{py}}\right|$
$\phi\left\{\frac{H_{ty}}{H_{py}}\right\}$
$\left|\frac{H_{ty}}{H_{py}}\right|$
$\phi°$
km
W
2 Ωm
400 Ωm
E

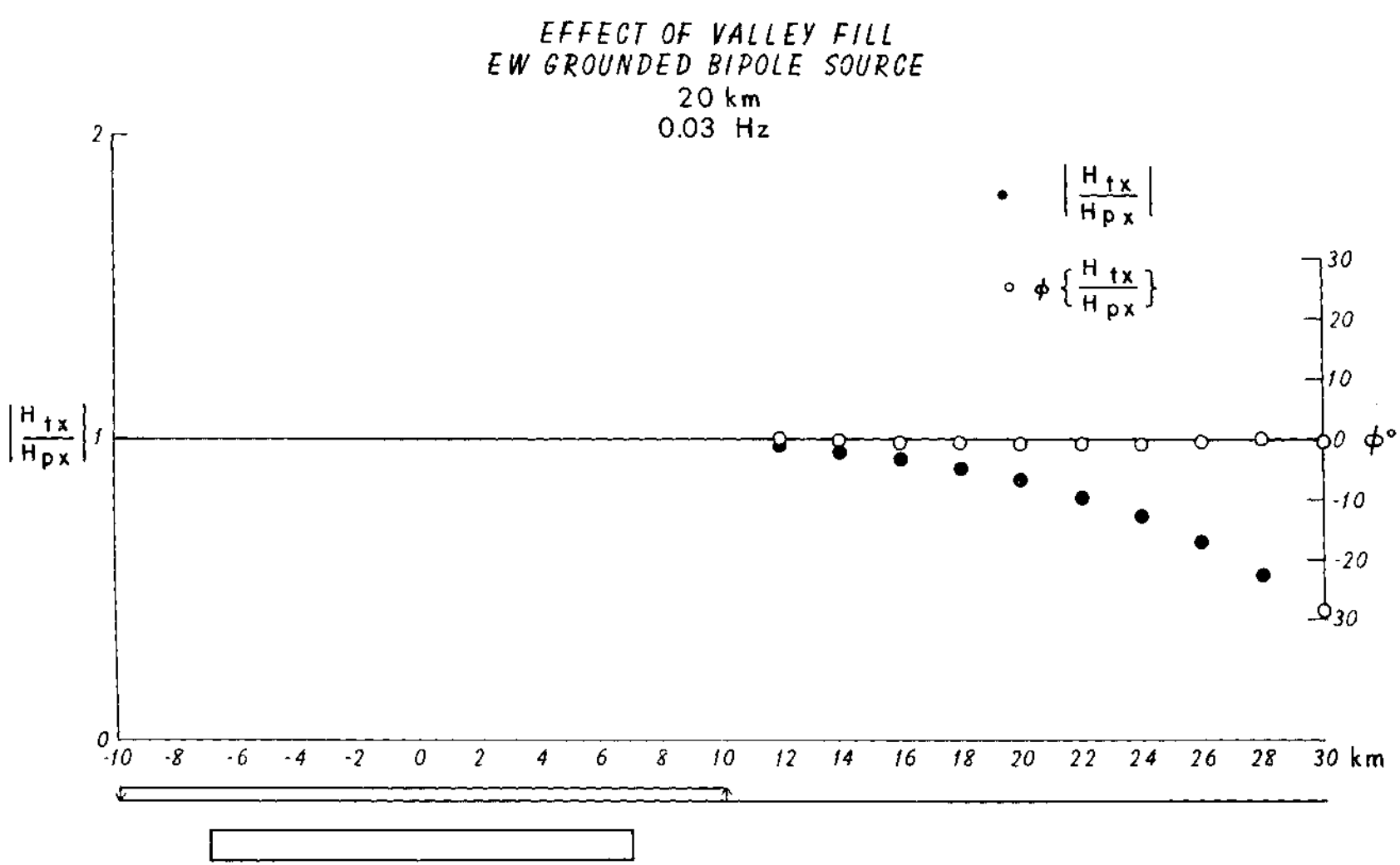
EFFECT OF VALLEY FILL
EW GROUNDED BIPOLE SOURCE
20 km
0.03 Hz
$\left|\frac{H_{tx}}{H_{px}}\right|$
$\phi\left\{\frac{H_{tx}}{H_{px}}\right\}$
2
1
0
30
20
10
0
-10
-20
-30
$\phi°$
-10 -8 -6 -4 -2 0 2 4 6 8 10 12 14 16 18 20 22 24 26 28 30 km